A Study of Dry Spells in Iran Based on Satellite Data and Their Relationship With ENSO

Mohammad Rezaei (mohammad.rezaey@modares.ac.ir)
Tarbiat Modares University https://orcid.org/0000-0001-7380-4665
Efi Rousi
Member of the Leibniz Association
Elham Ghasemifar
Tarbiat Modares University
Ali Sadeghi
Farhangian University

Research Article

Keywords: MCDDs, dry spells, satellite data, linear trend, ENSO, Iran

Posted Date: March 2nd, 2021

DOI: https://doi.org/10.21203/rs.3.rs-256310/v1

Version of Record: A version of this preprint was published at Theoretical and Applied Climatology on April 9th, 2021. See the published version at https://doi.org/10.1007/s00704-021-03607-y.

Abstract

The study of Maximum number of Consecutive Dry Days (MCDDs) is one approach to analyse precipitation behavior in arid and semi-arid regions of Iran. This study is a first attempt to investigate the MCDDs and their relationship with the El Niño/Southern Oscillation (ENSO) in winter months over Iran. The study was carried out using Tropical Rainfall Measuring Mission (TRMM) satellite data on a daily basis at 1° latitude × 1° longitude spatial resolution and reanalysis data for the period 1998-2019. Results showed that the highest values of MCDDs are observed in southeastern Iran and the lowest in northwestern Iran. Based on the coefficients of the linear trend of the MCDDs, the significant increasing trends are remarkably more abundant than declining trends, especially in the northern half of the country in December and January. The results regarding the relationship between ENSO and MCDDs indicated a non-stationary behavior, with significant negative correlation for December (especially in southwest) and positive correlation for January and February (especially in southeast). The largest differences in the correlation coefficients were observed between December and January. In general, during El Niño (La Niña) phases, the length of MCDDs decreases (increases) in December and increases (decreases) in January especially in the southern half. By comparing different large-scale climate parameters for the two months, we found that during El Niño (La Niña) phases, a negative (positive) anomaly of geopotential height, and a positive (negative) anomaly of zonal wind and specific humidity are observed over the region in December, while the opposite situation occurs in January. The innovation of this study is the use of satellite data that provide a continuous spatial coverage of the region and the consideration of the ENSO teleconnection pattern in regards to dry spells. We find that El Niño (La Niña) has contradictory effects on MCDDs in different winter months in the southern half of the country. These findings are of great importance for a country like Iran that lies in arid and semi-arid regions, as they can be useful for water resources management.

Introduction

The increase in anthropogenic greenhouse gas concentrations has led to drying conditions in the Northern Hemisphere subtropics and tropics (Zhang et al., 2007; Min et al., 2011). During recent decades, precipitation has tended to decrease in the Northern Hemisphere subtropical zones (IPCC, 2007). The changes in precipitation regime had significant effects on arid and semi-arid regions, such as Iran.

One approach towards understanding precipitation characteristic is the study of dry spells, which gives a better characterization of the dry season than the sum of precipitation amount (Douguedroit, 1987). The dry spells are defined as a number of consecutive days without precipitation that affect extended areas (Anagnostopoulou et al., 2003; McCabe et al., 2010). In definitions of dry spells, there are various precipitation per day thresholds. Martin-Vide and Gomez (1999) used that of daily rainfall more than or equal to 10 mm threshold. Other studies used different threshold values such as 0.1, 1 and 10 mm (Kutiel, 1985; Kutiel and Maheras, 1992; Anagnostopoulou et al., 2003), and more than or equal to 5 mm (Serra et al., 2006; Lana et al., 2008). Dry spells may greatly affect soil moisture, snowpack, streamflow, groundwater, reservoir storage, and bring devastating damage to crops (Seleshi et al., 2006; Caloiero et al., 2015). The study of the occurrence of dry spells is therefore important in managing water resources and understanding the impact of climate change on droughts (Singh and Ranade, 2010; Deni et al., 2010; Llano and Penalba, 2011).

Several previous studies investigated the trend of dry spells in various parts of the world and obtained contradictory results in spatial and temporal scales. Seleshi and Camberlin (2006) found no trends in the yearly maximum length of dry spells over Ethiopia. Many studies have observed a decreasing trend in dry spell periods in the winter season, such as Suppiah and Hennessy (1998) in Australia, Serra et al. (2006) in Catalonia (Spain), Deni et al. (2010) over Peninsular Malaysia, McCabe et al. (2010) in the southwestern United States, Duan et al. (2017) in China,. On the contrary, some studies observed an increasing trend in winter dry days, for example, Schmidli and Frei (2005) in Switzerland, Sang et al. (2015) in Peninsular Malaysia, and Caloiero et al. (2015) in southern Italy.

Numerous studies have reported a significant relationship between dry spells and teleconnection patterns in different parts of the world (Bonsaland Lawford, 1999 in the Canadian Prairies; Barrucand et al., 2007 in Argentina; Oikonomou et al., 2010 in Eastern Mediterranean; Unalet al., 2012 in Turkey; Wang et al., 2015 in the arid region of China; Raymond et al., 2018 over the Mediterranean basin).

Several studies have been performed regarding precipitation trends in Iran. Modarres and Sarhadi (2009) found that negative trends of annual rainfall are mostly observed in northern and northwestern regions. Tabari and Talaee (2011) showed that significant negative trends occurred mostly in the northwest of Iran. Abarghouei et al. (2011) indicated a significant negative trend of drought in many parts of Iran, especially the southeast, west and southwest regions of the country. Some'e et al. (2012) showd decrease in the winter precipitation series in northern Iran, as well as along the coasts of the Caspian Sea. Raziei et al. (2014) found that the precipitation is

decreasing in spring and summer and increasing in autumn and winter in most of Iran. Najafi and Moazami (2016) showd an overall declining trend of the annual precipitation, in particular in regions located on the north, west and northwest of Iran. The seasonal analysis shows the largest contribution of winter to this declining trend. Asakereh (2017) indicated that there were major declining changes in precipitation in the northwest of Iran. Numerous studies showed a significant relationship between precipitation in Iran and various teleconnection patterns such as SOI (Nazemosadat and Cordery, 2000.a; Nazemosadat and Cordery, 2000b; Araghi et al., 2016; Dehghani et al., 2020), ENSO (Mariotti, 2007; Hosseinzadeh et al., 2014; Biabanaki et al., 2014); Alizadeh-Choobari et al., 2018), the NAO (Dezfuli et al., 2010; Araghiet al., 2016), AO (Araghi et al., 2016), the PDO (Biabanaki et al., 2014) and the SCN pattern (Ahmadi et al., 2019).

The results of a study of MCDDs are different compared to rainfall. Sivakumar MVK (1992) and Cindrić et al. (2010) pointed out that relying only on the precipitation amount can sometimes lead to incorrect conclusions because if heavy precipitation is recorded after a long dry spell, one might assume that the analyzed period was wet, while this was not the case. For Iran, Nasri and Modarres (2009) revealed individual trends of dry spells in the Isfahan Province, however so far no comprehensive study has been conducted in this regard.

One of the benefits of this research is the use of precipitation from satellite data. The advantage of satellite data is that they have full spatial coverage and can also provide data for Iranian deserts (which do not have meteorological stations). Recent findings by Brocca et al. (2020) indicated that, particularly over scarcely gauged areas, integrated satellite products outperform both ground- and reanalysis-based rainfall estimates. Additionally, Darand et al. (2017) showed that the TRMM precipitation data in Iran has high potential in regions where rain gauge observations are nonexistent. Therefore, this study is the first comprehensive study on MCDDs over Iran. The results of this research are presented in three separate sections. First, we focus on the spatial characteristics of the MCDDs over Iran. Then, the results obtained from the MCDDs trend analysis are presented and finally, the relationship between the MCDDs and the ENSO teleconnection pattern is examined.

Study area

Iran is located in the subtropical arid belt of the northern hemisphere and covers an extensive area of 1648000 km2 (Fig. 1, left panel) (Hosseinzadeh, 2004; Modarres, 2006). The annual rainfall in Iran is 250 mm, that is less than the global average (Raziei et al., 2014). The two major mountain ranges in Iran are Alborz in the north and Zagros in the west, while the main deserts of Iran are Dasht-i-Kavir and Dashte- Lut (Shenbrot et al., 1999). In this study, the satellite precipitation data obtained are based on 156 1° latitude × 1° longitude grid points within the Iran borders (Fig. 1, right side). In order to better interpret the results in different geographical regions of Iran, we divided the country into 4 parts based on gridded points, including Northwest (NW), Northeast (NE), Southwest (SW) and Southeast (SE). This division was made due to the diversity of Iran's climate in these areas and it is helpful for a better presentation of the results.

Data And Methods

In this study, we obtained 22 years (1998 to 2019) of daily precipitation data from TRMM (3B42_Daily v7) for winter months (Dec, Jan, Feb and Mar) from the Giovanni interface (http://giovanni.gsfc.nasa.gov/giovanni/). The reason for choosing the winter months was due to the fact that more than half of the annual precipitation in Iran occurs during this season (Domroes et al., 1998). The TRMM rainfall data were resampled to a 1° spatial resolution and considering the one-degree distance, 156 points were examined (Fig. 1, right side). Then, the MCDDs were calculated for each of the winter months from December to March. In this study, the MCDDs are defined as the longest period of consecutive days, during which no precipitation occurred. After extracting the MCDDs for all points, their temporal and spatial characteristics were examined separately for each month. In the next step, the magnitude of trends was derived using linear regression. Finally, the Spearman correlation was used in order to measure the relationship between the MCDDs and the ENSO teleconnection pattern. The teleconnection pattern index used in this study is the multivariate ENSO index, which was obtained from the Climate Prediction Center website (http://www.cpc. ncep.noaa.gov/data/teledoc/telecontents.shtml).

As we wanted to observe whether there is spatial homogeneity in the correlation coefficients between the ENSO and MCDDs, the spatial autocorrelation index was used. Spatial autocorrelation is the correlation among values of a single variable with itself in geographic space (Griffith 2003). The spatial autocorrelation can be calculated by various spatial statistics such as Moran's I (Moran, 1950) that was used here:

$$(1)\ I = \frac{\sum_{i=1}^{n}(x_i - \bar{x})\sum_{j=1}^{n} w_{ij}(x_j - \bar{x}) / \sum_{i=1}^{n}\sum_{j=1}^{n} w_{ij}}{\sum_{i=1}^{n}(x_i - \bar{x})^2 / n}$$

Where x_i is the observed correlation coefficient at point i, x is the average of all correlation coefficients over the n points, and wij is the spatial weight between two points i and j. Here wij takes a nonzero value if the two locations are neighbors and zero otherwise. In the right-hand part of Eq. (1), all weights are stored in the spatial weight matrix. In this study, the spatial autocorrelation will be referred to as Moran's I. Moran's I values vary between −1 and 1. Values of Moran's I larger than expected (perfect positive correlation) mean that values tend to be similar and values smaller than expected (perfect positive correlation) reveal that they tend to be dissimilar (Griffith 2003).

After calculating the correlation coefficient, the points with the most significant values were identified. Then, the relationships between MCDDs and atmospheric variables, such as Sea Level Pressure (SLP), geopotential height, wind and specific humidity were investigated.For this, reanalysis data from the NCEP/NCAR (National Centers for Environmental Prediction/National Center for Atmospheric Research) were used (Kalnay et al., 1996). To investigate the effect of ENSO on the MCDDs anomalies, the strongest El Niño and La Niña years were identified separately for each month (Table 1), and mean anomaly maps were compared for each phase . The 5 strongest El Niño (La Niña) years were obtained after sorting the ENSO index to compare the MCDDs lengths during the most pronounced warm and cold phases. Anomalies of MCDDs and reanalyses data for each month were calculated using Z-scores.Then the monthly average of standard scores for the years of ElNiño and LaNiña was calculated (see Table 1 for the years used in each case).The aim is to find out whether there is a significant difference between the values of MCDDs, as well as of the different atmospheric variables, when comparing the El Niño and La Niña phases. For this purpose, a one-way analysis of variance was used. A paired t-test was performed to compare the differences in MCDDs lengths between all 22 years and the 5 El Niño (La Niña) years and calculate the statistical significance.

Table 1- The strongest phases of Enso (El Niño and La Niña) in different years separately for each month.

Mar	Feb	Jan	Dec	Month
1998-2005-2010-2016-2019	1998-2003-2005-2010-2016	1998-2003-2007-2010-2016	2002-2004-2006-2009-2015	**El Niño**
1999-2000-2008-2009-2011	1999-2000-2001-2008-2011	1999-2000-2008-2011-2012	1998-1999-2007-2010-2011	**La Niña**

Results And Discussion

The distribution of average monthly MCDDs

Fig. 2 shows the mean monthly MCDD length for each grid point in Iran (grid points with high standard deviation are marked) Dec to Mar for the study period 1998-2019. As mentioned, in order to better analyze the spatial distribution of MCDDs, Iran is divided into four separate regions: the northeast, northwest, southeast and southwest.In general, the monthly maximum and minimum average MCDDsis observed during Dec (15.8±6.4) and Feb (12.8±5.2), respectively. Table 2 presents some of the statistical characteristics of the MCDDs values from Dec to Feb for the4 geographical regions of Iran.

In Dec, the maximum and minimum spatial values of MCDDs are observed in the southeastern (20.4 ± 7.6) and in the northwest region (11.7±4.7), respectively. During Dec the maximum amount of MCDDs is observed on the southeastern region (MCDDs= 26.5) (at latitude 27.5° and longitude 60.5 °), while the minimum value is located in northeastern Iran (MCDDs= 6.9) (at latitude 36.5° and longitude 54.5 °). In January, the maximum and minimum spatial values of MCDDs are observed in the southeast (17.9±6.7) and in the northwest (12.6 ±5.5), respectively. In this month, the amount of MCDDs in the southwestern region of Iran is 12.8 (5.5). Therefore, in January, there is no significant difference between the northwestern and southwestern regions of Iran. In general, MCDDs in the western half are fewer, compared to the eastern half. In January the maximum amount of MCDDs was observed on the southeastern

region (MCDDs= 24.6) (at latitude 31.5° and longitude 58.5 °), while the minimum value is located in southwestern Iran (MCDDs= 7.8) (at latitude 31.5° and longitude 50.5 °). In Feb, the maximum and minimum spatial values of MCDDs are observed in the southeast (15.9±6.4) and in the northwest (10.9 ±4.6), respectively .During Feb the maximum amount of MCDDs was observed in the southeastern region (MCDDs= 21.1) (at latitude 25.5° and longitude 59.5 °), while the minimum value is located in northwestern Iran (MCDDs= 6) (at latitude 34.5° and longitude 47.5 °). Finally, in March, similarly to previous months, the maximum and minimum spatial values of MCDDs are observed in the southeast (17±6.7) and in the northwest (9.6 ±4.2) ,respectively. During March the maximum amount of MCDDswas observed on the southeastern region (MCDDs= 21.8) (at latitude 27.5° and longitude 61.5 °), while the minimum value is located in northwestern Iran (MCDDs= 4.2) (at latitude 34.5° and longitude 47.5 °).

Based on the above results, the highest (lowest) values of MCDDs occur in the southeast (northwest) in all months. This is in contrary to the findings of drought-related research but similar to the results obtained from the distribution of rainfall values in Iran. Bazrafshan and Khalili (2013) showed that drought phenomena can occur both in the northwest and in the southeast of the country. According to the study of Ashraf et al. (2014) Rasht (at the southern Caspian Sea) had the highest and Yazd (at the Southeast region in this study) had the lowest amount of total precipitation over Iran.In general, the frequency of rainy days in southeastern Iran is low and vice versa in the northwest, especially at the southern shores of the Caspian Sea, where the frequency of occurrence is very large.Nazaripour and Daneshvar (2014) reported that one-day precipitationgenerates the maximum annual precipitation amounts in eastern parts of Iran. Raziei et al. (2014) showed that the maximum number of rainy days are observed in the Caspian Sea region.

Table 2- Characteristics of descriptive statistics of MCDDs in the geographical areas of Iran separately for each month.

Month	Region	Mean	SD	Max	Min
Dec	SW	14.4	6.5	19.1	9.2
	SE	20.4	7.6	26.5	11.5
	NW	11.7	4.7	18.0	7.7
	NE	16.6	6.7	22.6	6.9
	All	15.8	6.4	26.5	6.9
Jan	SW	12.8	5.5	17.1	7.8
	SE	17.9	6.7	24.6	8.5
	NW	12.6	5.5	16.0	7.9
	NE	14.5	5.6	18.7	8.9
	All	14.5	5.8	24.6	7.8
Feb	SW	11.3	4.8	15.4	6.9
	SE	15.9	6.4	21.1	6.2
	NW	10.9	4.6	14.7	6.0
	NE	13.1	5.3	17.0	8.5
	All	12.8	5.2	21.1	6.0
Mar	SW	12.2	5.2	16.1	5.9
	SE	17.0	6.7	21.8	6.3
	NW	9.6	4.2	16.1	4.2
	NE	13.8	5.5	19.8	5.5
	All	13.2	5.4	21.8	4.2

Analysis of MCDDs trend

In Fig. 4, the positive and negative coefficients of the linear trend are mapped for the months of Dec to Mar. In general, the average coefficients from Dec to Mar are 0.18, 0.25, 0.17, and 0.08, respectively. In all months, the frequency of points with positive coefficients is significantly higher than that of points with negative coefficients. The number of points with positive (negative) coefficients for January to March is 121 (33), 133 (22), 137 (16), and 105 (49), respectively. Fig. 4 shows the points with a significant trend along with their coefficients of determination. The number of points with a significant trend of the MCDDs in Iran for Dec to Mar is 33, 38, 22 and 13, respectively. In all months, the highest number of points with a significant trend in the MCDDs are observed in northwestern and southeastern Iran. For example, during Dec, 18 points (with a one-degree spatial resolution) had a significant increasing trend in the northwest, while in the same month, 14 points had a decreasing trend in the southeast region.

These results are exactly in line with the findings of Golian et al. (2015). They showed that the northern, northwestern, and central parts of Iran have significant drying trends, while, there is no statistically significant drying trend in the eastern part of the country. In general, statistical significant trends in the MCDDs are more concentrated in the northern half of the country (especially in NW) than in the southern half. This is similar to previous results obtained for precipitation trends over Iran. Modarres and Sarhadi (2009); Tabari and Talaee (2011); Some'e, et al. (2012); Najafi and Moazami (2016) and Asakereh (2017) all found decreasing trends of precipitation in northern and northwestern regions.

In December, an increasing trend in the number of MCDDs can be seen in all regions of the country. The highest and lowest values of the average coefficients were observed in the northwest (0.25) and southeast (0.04), respectively. In this month, the highest value of the coefficient is 0.64 in the center of Iran (at latitude 32.5° and longitude 54.5 °, Fig.3.a) and its lowest value is -0.53 in southeastern Iran (at latitude 31.5° and longitude 60.5 °). In January, the spatial pattern of the coefficients is similar to December. MCDDs have an increasing trend in most parts of the country. In general, the average trend coefficient in southwestern Iran is higher than in other regions (0.32). Significant declining trends are also confirmed in the southeast, and significant increases are observed in parts of the central, southeastern, and western regions. Fig.3, b shows the increasing trend with coefficient 0.43, at latitude 28.5° and longitude 51.5°. In February, the number of points, which have a decreasing trend, reach the minimum number. However, in some points of the southeast, there is a decreasing trend in the MCDDs. In other parts of the country an increasing trend in the MCDDs can be seen during Feb. Fig.3, c shows the point with the maximum increasing trend (R2= 0.33) in the central region of Iran (at latitude 34.5° and longitude 54.5°). Finally, in Mar, similar to the previous months, there is a decreasing trend in the southeastern region and an increasing trend in other parts of the country. Significant trends are concentrated in the central parts of the country as well as in some parts of the southeast and west of Iran. During Mar, the highest value of the coefficient is 0.32 in the center of Iran (at latitude 33.5° and longitude 51.5 °, Fig.3.d).

The relationship between MCDDs and ENSO

In Fig. 5, the values of the correlation coefficients between MCDDs and the ENSO teleconnection pattern are mapped. As can be seen in the map, the significant correlation coefficients are negative in December and March, but positive in January and February.

In Table 3, the Moran's I values for the spatial correlation coefficients between the MCDDs and ENSO are presented separately for each month.The Moran's I can show how the values of the correlation coefficients are distributed spatially (in Fig 5). Low values of Moran's I show that the positive and negative correlation coefficients are irregularly distributed over the country, which means that it cannot be said that the ENSO has the same effect on the MCDDs variation during various months. Next, the relationships between MCDDs and ENSO values have been investigated in the winter months.

Table 3.Moran's Ivalues for correlation coefficients between MCDDs and the ENSO teleconnection pattern

Month	Dec	Jan	Feb	Mar
Moran I	0.16	0.19	0.39	0.35

In December, the ENSO showed an inverse relationship with MCDDs in southwestern Iran, but regarding the value of Moran index (0.16), its effects have a low spatial homogeneity compared to other months. In December, all significant correlation coefficients are negative and are often located in the southwestern region. In January, the Moran value is 0.19. The average correlation coefficients in the southeast (0.15) are higher than in other regions and the maximum is 0.57. The Moran's index in February shows that the spatial homogeneity of the correlation coefficients is higher compared to the other months. In the northeast and southwest, the coefficients are mostly positive. For example, in the southwest, the average correlation coefficient is 0.25. However, in the southeast and northwest,

several points have a negative coefficient.As mentioned, in February, the relationship between MCDDs and the ENSO index is often positive in different parts of Iran. The positive and significant correlation coefficients are observed from southwest to northeast.

The length of the MCDDs has also increased as the value of the ENSO index increases. In February, there is also a negative correlation in some parts of the southeast and northwest. The strongest coefficient can be seen at latitude 37.5° and longitude 45.5 °, (r = -0.57). According to the correlation coefficient values, during February the lowest and highest amount of relationship between the ENSO index and MCDDs were obtained in southwest at latitude 30.5° and longitude 53.5 ° (r =0.66), and in northwest at latitude 36.5° and longitude 47.5 ° (r= -0.57), respectively.In March, the Moran coefficient is 0.35 and the ENSO has an effect on the amount of MCDDs. In general, in most parts of Iran, there is a negative relationship (r = -0.15) and its highest is -0.69. Also, in the northwest, the average coefficients are negative (r = -0.02), but this relationship is weaker than in other regions. The positive ENSO values are related to El Niño events (warm phase) which is connected to wetter conditions over most regions of Iran according to various studies (Nazemosadat et al., 2000,a; Hosseinzadeh Talaee et al., 2014; Biabanaki et al., 2014; Alizadeh-Choobari et al., 2018; Ahmadi et al., 2019). Indeed, it is found that in the warm phases of ENSO, the length of the MCDDs has decreased, which is consistent with previous studies. The negative coefficients are more abundant in December than in other months. Mariotti (2007) reveals that the ENSO impact on precipitation of southwest Asia is highest during the transition seasons of autumn and spring.In March, the lowest and highest amount of the relationship between the ENSO index and MCDDs was obtained in the south (at latitude 28.5° and longitude 53.5 °, r = -0.69), and in the northeast (at latitude 37.5° and longitude 57.5 °,r= 0.37), respectively. Table 4 shows the average and maximum correlation coefficients between MCDDs and ENSO for the four different regions.

Table 4- Mean and maximum values of the correlation coefficients between MCDDs and ENSO in the 4 geographical areas of Iran and over the whole country.

Month	Region	ENSO vs. MCDDs	
		Mean	Max
Dec	SW	-0.33	-0.59
	SE	-0.21	-0.61
	NW	-0.12	-0.46
	NE	-0.19	-0.65
	All	-0.20	-0.65
Jan	SW	0.05	-0.41
	SE	0.15	0.57
	NW	0.03	-0.60
	NE	0.14	0.50
	All	0.11	-0.60
Feb	SW	0.25	0.58
	SE	0.02	0.66
	NW	-0.01	-0.57
	NE	0.17	0.49
	All	0.08	0.66
Mar	SW	-0.10	-0.46
	SE	-0.29	-0.69
	NW	-0.02	-0.45
	NE	-0.08	0.39
	All	-0.15	-0.69

Comparison of MCDDs anomalies in El Niño and La Niña periods

In the previous section, it was observed that the effect of the Multivariate ENSO Index (MEI) on the MCDDs varibility can differ from one winter month to another. We calculated the correlation coefficients between the MCDDs and other ENSO indicators such as Niño 1+2, Niño 3.4, Niño 4 and SOI. In all cases, this contradiction was observed (not shown). In this section, the MCDDs anomalies in the five years with negative phase (La Niña) and the five years with positive phase (El Niño) are compared separately for each month (Fig. 6). The results of analysis of variance showed that there is a significant difference between the anomaly of MCDDs when comparing each month separately in the El Niño and La Niño phases (Table 5 and 6). In December, the average anomaly (in Iran) in the El Niño and La Niña phases is -0.45 (± 0.29) and 0.25 (± 0.33), respectively. This indicates that in the warm phases of ENSO the length of the MCDDs was shorter than in the cold phases. In January, the average anomalies in the El Niño and La Niña phases were 0.11 (± 0.35) and -0.24 (± 0.37), respectively. Therefore, in the warm phases of El Niño, not only has the length of dry periods not decreased, but it has also had a positive anomaly. In February, the situation is the same as in January. In the El Niño phases, the anomaly value is very small, 0.09 (± 0.35), but in the La Niña phases, the anomaly value is -0.2 (± 0.34) . In March, the anomalies were positive in both El Niño and La Niña phases. However, the amount of anomaly in El Niño (0.08, ±0.38) is insignificant compared to La Niña (0.33, ±0.41). In Fig. 6, the black circles on the MCDDs anomaly values show the points with statistical significant differences (at the 5% level) between the long-term (22 years) MCDDs values compared to the their values during El Niño and La Niña phases based on the t-test. In the El Niño years, the most significant differences are observed for December (at 32 points) from southwest to northeast, but in the other months the number of significant points is very small. However, significant differences can be seen in all months in the La Niña years. The significant differences are negative in January and February but positive in December and March. Therefore, the contradiction in the MCDDs length (between January-February with December-March) is stronger during the La Niña compared to the El Niño periods.

These results are consistent with the results obtained from the correlation coefficients and they confirm the contradiction of the relationship between MCDDs and ENSO in January-February compared with December-March. Therefore, in terms of the MCDDs anomalies, in general, January and February have a positive relationship, and December and March have a negative relationship with the ENSO index. The largest differences in correlation values between the El Niño and La Niña phases are observed for December (0.71) and January (-0.35), respectively. In addition, in the El Niño phases, there is a difference between the anomaly values in different months, with the most significant difference between January and December (0.56). However, the difference between January and February in the years of El Niño is negligible (-0.01) (Table 5).

Table 5 shows the average of MCDDs anomalies during El Niño and La Niña years separately in different geographical areas of Iran. As can be seen in the table, during El Niño years, negative anomalies are observed only in December in all areas. But the amounts of MCDDs anomalies in January, February, and March are often positive. The greatest difference can be seen between December (-0.67) and February (0.47) in southwestern Iran. In the La Niña years in December and March, there are positive anomalies in all regions, but stronger in the southern half (positive anomalies are very weak in the northwest), while in January and February, the negative anomalies are predominant in the country (except in the northwest). The greatest differences in anomalies can be seen between January (-0.31) and March (0.55) in the southeast.

In La Niña phases, there is also a significant difference between anomalies in different months. The highest and lowest differences can be seen for March and January (0.57) and February-January (0.03), respectively (Table 6). In the following steps, for better analysis, the anomalies of the atmospheric data were analyzed for January and December only and separately for the El Niño and La Niña phases.

Table 5- Average of MCDDs anomalies during El Niño and La Niña years separately in the four geographical areas of Iran.

Region	El Niño				La Niña			
	Dec	Jan	Feb	Mar	Dec	Jan	Feb	Mar
SW	-0.67	-0.16	0.47	0.22	0.31	-0.29	-0.24	0.22
SE	-0.45	0.22	0.05	-0.05	0.35	-0.31	-0.18	0.55
NW	-0.3	0.05	-0.03	0.22	0.15	-0.00	-0.04	0.09
NE	-0.5	0.14	0.1	0.09	0.16	-0.34	-0.38	0.28

Anomalies of large-scale atmospheric variables in El Niño and La Niña periods

According to the results obtained in the previous sections, the correlation coefficients as well as the anomalies of MCDDs in the El Niño and La Niña periods in December and January showed opposite results. In this section, to further analyze the cause of this contradiction, the anomalies of large-scale atmospheric variables in the El Niño (Table 6) and LaNiña (Table 7) periods for December and January are compared over Iran. In addition, the anomalous values are presented as a pairwise comparison between different winter months. However, for brevity, comparisons have been only made between January and December.

Table 6- Anomaly comparison of MCDDs and large-scale variables in El Niño between winter months.

variable	Month	Mean	SD	diff					
				Jan- Dec	Feb -Dec	Mar- Dec	Feb-Jan	Mar- Jan	Mar- Feb
MCDDs	Dec	-0.45	0.29	0.56**	0.55**	0.54**	-0.01	-0.02	-0.01
	Jan	0.11	0.35						
	Feb	0.09	0.35						
	Mar	0.08	0.38						
SLP	Dec	0.09	0.18	0.14	-0.17**	-0.08	0.31**	-0.23*	0.08
	Jan	0.23	0.35						
	Feb	-0.07	0.05						
	Mar	0.00	0.26						
hgt-500	Dec	-0.92	0.13	1.4**	0.72**	0.96**	0.66**	-0.47**	0.18**
	Jan	0.51	0.09						
	Feb	-0.14	0.05						
	Mar	0.04	0.12						
Uwnd-500	Dec	0.09	0.53	-0.29*	-0.18	0.13	-0.11	0.43**	0.31**
	Jan	-0.2	0.46						
	Feb	-0.08	0.04						
	Mar	0.23	0.08						
vwnd-500	Dec	0.49	0.57	-0.13	-0.22	-0.31**	0.08	-0.18	-0.09
	Jan	0.36	0.21						
	Feb	0.27	0.06						
	Mar	0.18	0.24						
shum-500	Dec	0.03	0.38	-0.06	0.00	0.64**	-0.07	0.71**	0.64**
	Jan	-0.03	0.43						
	Feb	0.04	0.24						
	Mar	0.68	0.18						

* * Significant at level of p=0.01 * Significant at the level of p=0.05

El Niño phases

As seen in Table 6, during the El Niño phases, the geopotential height at the 500 hpa level, as well as the zonal wind component at the same pressure level, show significant differences in December and January (within the borders of Iran). The maximum difference in

anomaly (1.4) is observed for the hgt-500. The 500-hpa negative anomalies in December and positive anomalies in January are seen in both the northern and southern half of the country (see Figure 7). As shown in Figure 6 (top row), the positive (negative) anomalies in MCDDs length are observed during January (December) in both northern and southern halves. This suggests that during El Niño periods in December, hgt-500 appears at a lower height compared to the long term climatology. This leads to more cyclones as well as reduced MCDDs over Iran. On the contrary, in January, a positive anomaly of the geopotential height indicates that cyclones are less frequent and MCDDs are longer. Alijani (2002) and Raziei et al. (2012) concluded that the spatial distribution of precipitation over Iran depends on the geographical position of the mid-tropospheric trough over the Middle East, which links to the results shown. The zonal wind direction component also has completely different values for December and January. In December, a positive anomaly is seen (especially in the southern half of the country), but in January, a negative anomaly can be seen in almost all of Iran. A higher zonal wind component in December indicates that the wind direction was mostly westerly. This leads to the passage of cyclones, the occurrence of more precipitation, and finally the reduction of the length of MCDDs. However, in January, the zonal wind magnitude was below normal. The difference between zonal wind anomalies in December and January is greater (difference = -0.97) in the southern half of the country, compared to the northern half (difference = 0.65). During the El Niño years, the zonal wind anomalies in the southern and northern halves are reversed in both January and December. In December (January), the zonal wind anomalies are negative -0.38 (positive 0.27) in the northern half and positive 0.44 (negative -0.53) in the southern half. Ghasemi and Khalili (2008) found a significant positive correlation between zonal winds and winter precipitation over most parts of Iran. The meridional wind component has a significant difference in December and January (difference = -0.32) in the southern half of Iran. Although the anomaly is positive in both months, the anomaly values in December are larger than in January. However, the meridional wind component does not differ significantly between December and January in the northern half. The anomaly values of specific humidity at 500 hpa are 0.03 and -0.03 in December and January, respectively. Although the average humidity anomaly is not significantly different for the whole of Iran, the positive anomaly (0.21) in southern half in December and the negative anomaly (-0.2) in January are more pronounced. Similar to specific humidity, SLP does not show a significant difference for the whole country. However, there is a significant difference in the southern half in January when a relatively strong anomaly is seen in SLPs (0.47), while a weak negative anomaly is observed in the northern half at the same time. In general, in the El Niño years, when comparing December and January, the amount of MCDDs, as well as the anomalies of the hgt-500, in the northern and southern half do not differ significantly. However, zonal and meridian wind, SLP and humidity have different anomalies in the northern and southern half. In Fig. 7 anomalies of SLP, hgt-500, 500-hPa zonal wind and humidity are shown for January and December for the El Niño phases. The negative anomaly at the hgt-500 and the positive anomaly in the zonal wind and humidity cause a decrease in the length of MCDDs in December during the El Niño periods. On the contrary, the hgt-500 is higher than normal in January, while zonal wind and humidity are lower than normal and this synoptic situation leads to an increase in MCDDs during El Niño.

Table 7- Anomaly comparison of MCDDs and large-scale variables in La Niña phases betwnn winter months.

variable	Month	Mean	SD	diff					
				Jan -Dec	Feb -Dec	Mar -Dec	Feb -Jan	Mar -Jan	Mar -Feb
MCDDs	Dec	0.25	0.33	-0.49**	-0.46**	0.07	0.03	0.57**	0.53**
	Jan	-0.24	0.37						
	Feb	-0.2	0.34						
	Mar	0.33	0.41						
SLP	Dec	0.07	0.14	-0.28**	-0.04	-0.64**	-0.23**	-0.35**	-0.59**
	Jan	-0.21	0.39						
	Feb	0.02	0.08						
	Mar	-0.57	0.33						
hgt-500	Dec	0.67	0.11	-1.39**	-0.85**	-0.8**	-0.54**	0.58**	0.04
	Jan	-0.72	0.08						
	Feb	-0.18	0.1						
	Mar	-0.13	0.04						
Uwnd-500	Dec	-0.34	0.22	0.58**	0.78**	0.26**	-0.19	-0.32*	-0.51**
	Jan	0.24	0.58						
	Feb	0.43	0.13						
	Mar	-0.07	0.15						
vwnd-500	Dec	-0.24	0.29	0.39**	-0.03	0.45**	0.43**	0.05	0.48**
	Jan	0.15	0.29						
	Feb	-0.27	0.24						
	Mar	0.21	0.12						
shum-500	Dec	-0.66	0.23	0.59**	0.18**	1.3**	0.41**	0.7**	1.1**
	Jan	-0.06	0.69						
	Feb	-0.48	0.2						
	Mar	0.63	0.05						

* * Significant at level of p=0.01 * Significant at the level of p=0.05

La Niña phases

In the negative cold phases of ENSO (La Niña), the atmospheric parameters have significant differences in December and January (within the borders of Iran). Those differences between December and January are larger in the La Niña periods than in the El Niño periods in consistent with the MCDDs anomalies (see also black circles in Fig. 6). The highest anomaly difference between December and January (within the borders of Iran) is observed for the hgt-500 (-1.39), the values of 500-hpa specific humidity (0.59), 500-hpa zonal wind (0.58) and 500-hpa meridonal wind (0.39). The500-hpa geopotential height for January and December during the La Niña years is exactly the opposite of the El Niño ones.

In the La Niña phases, the average anomaly at the hgt-500 for December and January is 0.67 and -0.72, respectively. This shows that in the La Niña periods during December, the hgt-500 is higher than the long-term situation, and vice versa, in January, it is lower than the long-term average in Iran (see also Fig. 8). The 500-hpa negative anomalies in December and positive anomalies in January are seen in both the northern and southern half of the country (see Figure 8). As shown in Figure 6 (bottom row), the negative (positive) anomalies in MCDDs length are observed during the January (December) in both the northern and southern halves. In the years of La

Niña, the 500-hpa zonal wind is completely different for December and January. In December, a negative anomaly (-0.34 ± 0.22) is seen in the zonal wind (except in a small part of the northwest). However, in contrast to the El Niño periods, a positive anomaly (0.24 ±0.58) was observed in January, especially in the southern half of Iran. This positive anomaly of the 500-hPa zonal wind in January indicates that the wind flow was mostly westerly, which leads to more cyclones, more precipitation, and a decrease in the length of the MCDDs. In December, however, the zonal wind has a negative anomaly, and this has led to an increase in the length of the MCDDs. The difference between zonal wind anomalies in December and January is significant only in the southern half (difference = 1.15). Similar to the El Niño years, the zonal wind anomalies are reversed in both January and December in the southern and northern halves during the La Niña years.

Unlike the El Niño years, during the La Niña periods, there is a significant difference in the values of the 500-hPa meridional wind. In December, the 500-hPa meridional wind has a negative anomaly (-0.24 ±0.29), while in January it has a positive anomaly (0.15 ±0.29). This shows that in the La Niña periods during December, the meridional wind often had a northward direction, while in January it often had a southward direction, which led to a decrease in the length of the MCDDs in December and an increase in January. The meridional wind component has a significant difference in December and January (difference = 0.46) in the southern half of Iran and the anomaly is the opposite of that in the El Niño years. This indicates that in January, the wind often tends to be southward during La Niña years in the southern half. Similar to the zonal wind, Ghasemi, A. R., &Khalili, D. (2008) found significant positive correlation between meridional winds and winter precipitation over most parts of Iran. The specific humidity anomaly is consistent with the wind direction and the geopotential height. In December, the 500-hpa specific humidity is negative in all regions of Iran (-0.66 ± 0.23). The negative specific humidity confirms the increase in the length of MCDDs in the La Niña phases for December. In January the specific humidity anomaly is positive in the southern half (0.35) and negative in the northern half (-0.76) and this leads to an average anomaly close to zero over the whole country. Finally, SLP does not show a significant difference in the northern half, but only in the southern half (diffrence= -0.54). In January, a relatively strong negative anomaly is seen in SLPs (-0.45), while a weak positive anomaly is observed in the northern half at the same time. Fig. 8 (similar to Fig. 7) compares the anomaly values of sea level pressure, the hgt-500, zonal wind and specific humidity in the years of La Niña for January and December. The positive anomalies at hgt-500 and negative anomalies in the 500-hPa zonal wind and specific humidity lead to an increase in MCDDs during the La Niña periods in December. However, in January, the hgt-500 has a negative anomaly, and at the same time, the 500-hPa zonal wind and the specific humidity present a positive anomaly. These factors combined lead to a decrease in the duration of MCDDs in January in the La Niña periods.

Consistency analysis in anomalous values

In the previous section, anomalous values for the El Niño and La Niña years were examined as averages of 5 events occurring in different years (see Table 1). However, it is important to check the consistency of the anomalous values for each of the 5 El Niño and La Niña years. As shown in Table 5, in the El Niño years, the greatest differences in MCDDs anomaly values are observed between December (negative) and February (positive) in the southwest. Fig 9 shows the boxplots of MCDDs anomaly values and atmospheric variables during the La Niña and El Niño years. During the El Niño years of December (Fig 9a. green color boxes), there is consistency in the anomaly values of the MCDDS, the hgt-500, as well as the zonal wind in southwestern Iran. In particular, there are negative and positive anomalies in the hgt-500 and the zonal wind, respectively. In February during the El Niño years (Fig 9a. violet color boxes), there is consistency in the MCDDs anomalies (apart from 2003 when the MCDDs anomaly is negative and the whole situation is more similar to Dec 2002). The average MCDDs anomaly in the southwest is higher in comparison with other regions, but it is not very high (0.47). However, the largest anomaly is 1.1 at latitude 31.5° and longitude 51.5. Although zonal wind anomalies and specific humidity are mostly negative during the 5 El Niño events in the southwest, low consistency is observed among the atmospheric variables. As mentioned before, in the La Niña years, the greatest difference between January and March is observed in the southeast and this is why we present results for this region in Fig. 9. In January (Fig 9b. green color boxes), in all La Niña years, the average MCDDs anomaly is negative and the anomalies of the atmospheric variables are consistent with that. In four out of five La Niña years, the values of SLP and hgt-500 have negative anomalies, while the values of zonal wind and humidity have positive anomalies. Fig. 10 shows the anomalous values of atmospheric variables during January for each of the La Niña years separately. All atmospheric variables confirm that the MCDDs length decreases during La Niña in January in the southeastern region. Finally, in March, during La Niña years (Fig 9b. violet color boxes), there are consistently positive anomalies of MCDDs in the southeast. However, no stability can be observed in atmospheric variables.

Table 8 shows the correlation coefficients between the MCDDs with the ENSO index and the large-scale atmospheric variables for two points with the largest difference between MCDDs anomalies in the El Niño and La Niña phases in December (at latitude 28.5° and longitude 52.5) and January (at latitude 28.5° and longitude 54.5). Both grid points are located in the southwestern region. In January,

the MCDDs anomaly during El Niño and La Niña phases is 0.3 and -1.36, respectively, at latitude 28.5° and longitude 54.5. The correlation coefficient between SLP and MCDDs is positive but statistically insignificant (R= 0.3) at both selected points (Table 8). This is consistent with the results of previous studies. Mariotti (2007) showed that in the relationship between southwest central Asia rainfall and ENSO the role of SLP is insignificant. Instead, the moisture flux plays a more important role. As presented in Table 6, in January, during El Niño (La Niña) years, a positive (negative) anomaly is observed in SLP and hgt and vice versa, a negative (positive) anomaly in zonal wind and specific humidity. The MCDDs have a positive and statistically significant correlation with 850 and hgt-500. On the other hand, the correlations between MCDDs and zonal and meridional winds, as well as humidity, are negative. A similar relationship is seen between the ENSO index and the atmospheric parameters. For example, during the positive phases, the zonal winds and the humidity are decreased. In December, the MCDDs anomaly in El Niño and La Niña phases is -1.1 and 1.03, respectively, at latitude 28.5° and longitude 52.5. During El Niño (La Niña) years, a negative (positive) anomaly is observed in 850 and 500- hpa hgt and vice versa, a positive (negative) anomaly in zonal wind and specific humidity. Therefore, the situation in December is quite the opposite of that in January. The correlations between the MCDDs and the ENSO index and large-scale atmospheric variables are similar to the previously described grid point, but there is no significant correlation between MCDDs and SLP.

Nevertheless, the important point is that the relationship between ENSO and the 500-hpa hgt, 500-hpa zonal winds and humidity in December is quite the opposite of that in January. In January, the correlation coefficient between the ENSO and the 500-hpa specific humidity is negative and statistically significant (-0.69), while in December it is positive and significant as well (0.71, see Table 7). Fig. 11 shows three-dimensional scatter plots between atmospheric parameters (such as SLP, hgt-500, zonal winds and specific humidity), MCDDs and the ENSO index. In December, at latitude 28.5° and longitude 52.5 (shown with red colour in Figure 11), the relationship between ENSO, zonal winds and humidity is positive. On the contrary, during January at latitude 28.5° and longitude 54.5 (blue colour in Figure 11), ENSO has a negative relationship with those variables. Therefore, this indicates that the ENSO index does not have the same effect in January and December, proving the previously described non-stationary behavior.

Table 8- The comparsion of correlation coefficients between ENSO and MCDDs with large-scale atmospheric variables and anomaly values in two grid points in January and December.

location	comparison		SLP	Hgt		vwnd		uwnd		shum	
				850hpa	500 hpa	850hpa	500 hpa	850hpa	500 hpa	850hpa	500 hpa
54.5E_28.5N (Jan)	Anomaly	El Niño	0.74	0.79	0.4	-0.46	0.57	-0.64	-0.77	-0.34	-0.51
		La Niña	-0.95	-1.07	-0.51	0.67	0.19	0.45	0.91	0.9	1.01
	Cor	MCDDs vs.	0.3	0.48*	0.45*	-0.64**	-0.03	-0.1	-0.67**	-0.69**	-0.7**
		ENSO vs.	0.55**	0.55**	0.31	-0.47*	0.21	-0.23	-0.5**	-0.56**	-0.69**
52.5E_28.5N (Dec)	Anomaly	El Niño	0.02	-0.87	-0.98	0.5	0.77	0.3	0.78	0.61	0.5
		La Niña	-0.25	0.3	0.56	-0.34	-0.19	-0.79	-0.69	-0.84	-0.98
	Cor	MCDDs vs.	-0.16	0.55**	0.74**	-0.63**	-0.40*	-0.74**	-0.77**	-0.73**	-0.77**
		ENSO vs.	0.3	-0.31	-0.49*	0.44*	0.63**	0.53**	0.59**	0.7**	0.71**

* * Significant at level of p=0.01 * Significant at the level of p=0.05

Jet stream pattern

Precipitation anomalies are related with changes in the jet stream position (Belmecheri et al. 2017; Gaetani et al., 2011). Fig. 12 compares the jet stream patterns in the El Niño and La Niña years between January and December. In January, jet stream values are

weaker in the El Niño years (Fig. 12 c) compared to the La Niña years (Fig. 12 d) over Iran, and especially in the southern half of the country, where during La Niña the wind speeds exceed 45 m/s in this region. This is consistent with the results in the previous section that in the La Niña-January period the length of MCDDs is shorter in southeastern Iran (compared to El Niño periods). On the other hand, the jet stream pattern in December is completely opposite to that of January. In the El Niño periods (Fig. 12 a), wind speeds in the southern half are stronger than in the La Niña periods (Fig. 12 b). For this reason, in December, the MCDDs length is shorter during El Niño and especially in the southwest part of the country.

Conclusions

In this study, the characteristics of the Maximum Number of Consecutive Dry Days (MCDDs) were investigated using satellite data (TRMM- 3B42RT) for 1998-2019 on a daily basis in Iran. The major results obtained in this study are as follows:

1) The highest and lowest MCDDs values were observed in southeastern and northwestern Iran, respectively. The maximum and minimum spatial monthly average of MCDDs were observed during Dec (15.8±6.4) and Feb (12.8±5.2), respectively.

2) The analysis of the linear trends of the MCDDs indicated mostly positive coefficients in Iran. A significant increasing trend was observed in the MCDDs in all months and over the largest part of the country. However, a declining trend is dominant in some places in the southeastern region. The number of points with a significant trend of the MCDDs was more abundant in January and December. Also, spatially the highest number of points with a significant trend in the MCDDs was observed in northwestern and southeastern Iran.

3) The results of the correlation analysis between MCDDs and ENSO indicated that the effect of ENSO varies from month to month. In December and March, the relationship between MCDDs and ENSO is negative, but in January and February, the relationship is positive. Therefore, in the El Niño phases, the length of MCDDs increased in January (in the eastern half) and February (especially in the southwest), but decreased in December (especially in the southern half). These conditions are reversed in the La Niña phases. The analysis of the ENSO effect mechanism on MCDDs length showed that in each phase of El Niño and La Niña, there was a significant difference in the values of hgt-500, zonal wind, specific humidity and jet stream pattern between December and January, which explains why the effect on dry spells differs from one winter month to another. In particular, during El Niño (La Niña) phases, a negative (positive) anomaly of the geopotential height, and a positive (negative) anomaly of the zonal wind component and of the specific humidity were observed in December (January). This causes the length of MCDDs to increase (decrease) especially in the southern half in January (December) during the warm ENSO phases.

As seen in the results of this study, the largest differences between December and January seen in the effect of La Niña on dry spells over Iran, can be explained by the pronounced differences in the location and strength of the jet stream between the two months. In January the subtropical jet stream appears much more pronounced and located over the southern part of Iran, while in December the winds are very weak over the whole country. The reason why the jet stream response to La Niña is so different between December and January is a question that remains open and requires further dynamical analysis. According to Soulard et al. (2019), one of the factors modulating the jet is the AMO variability and Mohammadrezai et al. (2020) indeed found that AMO is important for drought over Iran. Also, as Iran lies in a region that is not always directly affected by ENSO conditions, it could be that there are other dynamical processes in play that define the response of dry spells even more than ENSO, or that the response is asynchronous and not simultaneous, as supported by Mohammadrezai et al. (2020). Furthermore, ENSO spatial variability is also very pronounced and it could be that different flavors of El Niño/La Niña (Johnson, 2013; Wiedermann et al. 2021) could trigger different remote effects on Iranian dry spells.

Therefore, based on satellite data that provide us with continuous spatial coverage over Iran, we find that El Niño (La Niña) has contradictory, non-stationary effects on MCDDs in different winter months, whereas previous studies have only referred to the positive (negative) effect of El Niño (La Niña) on Iranian rainfall in the autumn season. Hence, our findings can be useful in planning with regards to soil moisture, streamflow, groundwater and rainfed agriculture and thus of great importance for decision makers and stakeholders in Iran.

Declarations

-Conflict of Interest:

The authors declare that there are no conflicts of interest regarding the publication of this paper.

-Funding Statement:

The authors declare that there was no funding for the present study.

-Author's Contribution:

Mohammad Rezaei and Efi Rousi presented the initial idea of the work and supervised the study was Mohannad Rezaei and Efi Rousi. Elham. Gh and Ali S. helped us in statistical analysis. The final version is written by Mohammad Rezaei and Efi Rousi. The order of the authors is based on the level of their contribution.

-Availability of data and material:

The data that support the findings of this study are available from the corresponding author, upon reasonable request.

-Code availability:

The codes that support the findings of this study are available from the corresponding author.

-Ethics approval:

The authors declare that there is no human or animal participant in the study. Not applicable

-Consent to participate:

The authors declare that there is no human or animal participant in the study. Not applicable

-Consent for publication:

The authors give their consent to publication of all detailed of the manuscript including texts, figures and tables.

References

1. Abarghouei, H. B., Zarch, M. A. A., Dastorani, M. T., Kousari, M. R., &Zarch, M. S (2011) The survey of climatic drought trend in Iran. Stochastic Environmental Research and Risk Assessment, 25(6), 851.
2. Ahmadi, M., Salimi, S., Hosseini, S. A., Poorantiyosh, H., &Bayat, A (2019) Iran's precipitation analysis using synoptic modeling of major teleconnection forces (MTF). Dynamics of Atmospheres and Oceans, 85, 41-56.
3. Alijani, B (2002) Variations of 500 hPa flow patterns over Iranand surrounding areas and their relationship with the climate of Iran. Theoretical and applied climatology, 72(1-2), 41-54.
4. Alizadeh-Choobari, O., Adibi, P., &Irannejad, P (2018) Impact of the El Niño–Southern Oscillation on the climate of Iran using ERA-Interim data. Climate dynamics, 51(7-8), 2897-2911.
5. Anagnostopoulou C, Maheras P, Karacostas T, Vafiadis M (2003) Spatial and temporal analysis of dry spells in Greece. TheorApplClimatol 74:77–91.
6. Araghi, A., Mousavi-Baygi, M., Adamowski, J., & Martinez, C (2017) Association between three prominent climatic teleconnections and precipitation in Iran using wavelet coherence. International Journal of Climatology, 37(6), 2809-2830.
7. Asakereh, H (2017) Trends in monthly precipitation over the northwest of Iran (NWI). Theoretical and Applied Climatology, 130(1-2), 443-451.
8. Ashraf, B., Yazdani, R., Mousavi-Baygi, M., &Bannayan, M (2014) Investigation of temporal and spatial climate variability and aridity of Iran. Theoretical and Applied Climatology, 118(1-2), 35-46.
9. Barrucand, M. G., Vargas, W. M., &Rusticucci, M. M (2007) Dry conditions over Argentina and the related monthly circulation patterns. Meteorology and Atmospheric Physics, 98(1-2), 99-114.
10. Bazrafshan, J., &Khalili, A (2013) Spatial Analysis of Meteorological Drought in Iran from 1965 to2003. Desert, 18(1), 63-71.
11. Belmecheri, S., Babst, F., Hudson, A. R., Betancourt, J., & Trouet, V (2017) Northern Hemisphere jet stream position indices as diagnostic tools for climate and ecosystem dynamics. Earth Interactions, 21(8), 1-23.

12. Biabanaki, M., Eslamian, S. S., Koupai, J. A., Cañón, J., Boni, G., &Gheysari, M (2014) A principal components/singular spectrum analysis approach to ENSO and PDO influences on rainfall in western Iran. Hydrology Research, 45(2), 250-262.
13. Brocca, L., Massari, C., Pellarin, T., Filippucci, P., Ciabatta, L., Camici, S., ... & Fernández-Prieto, D (2020) River flow prediction in data scarce regions: soil moisture integrated satellite rainfall products outperform rain gauge observations in West Africa. Scientific Reports, 10(1), 1-14.
14. Bonsal, B. R., &Lawford, R. G (1999) Teleconnections between El Niño and La Niña events and summer extended dry spells on the Canadian Prairies. International Journal of Climatology: A Journal of the Royal Meteorological Society, 19(13), 1445-1458.
15. Caloiero, T., Coscarelli, R., Ferrari, E., &Sirangelo, B (2015) Analysis of dry spells in southern Italy (Calabria). Water, 7(6), 3009-3023.
16. Cindrić, K., Pasarić, Z., &Gajić-Čapka, M (2010) Spatial and temporal analysis of dry spells in Croatia. Theoretical and applied climatology, 102(1-2), 171-184
17. Darand, M., Amanollahi, J., & Zandkarimi, S (2017) Evaluation of the performance of TRMM Multi-satellite Precipitation Analysis (TMPA) estimation over Iran. Atmospheric Research, 190, 121-127.
18. Dehghani, M., Salehi, S., Mosavi, A., Nabipour, N., Shamshirband, S., &Ghamisi, P (2020) Spatial Analysis of Seasonal Precipitation over Iran: Co-Variation with Climate Indices.
19. Deni, S. M., Suhaila, J., Zin, W. Z. W., &Jemain, A. A (2010) Spatial trends of dry spells over Peninsular Malaysia during monsoon seasons. Theoretical and applied climatology, 99(3-4), 357.
20. Dezfuli, A. K., Karamouz, M., &Araghinejad, S (2010) On the relationship of regional meteorological drought with SOI and NAO over southwest Iran. Theoretical and applied climatology, 100(1-2), 57-66.
21. Domroes, M., Kaviani, M., & Schaefer, D (1998) An analysis of regional and intra-annual precipitation variability over Iran using multivariate statistical methods. Theoretical and Applied Climatology, 61(3-4), 151-159.
22. Douguedroit, A (1987) The variations of dry spells in Marseilles from 1865 to 1984. Journal of Climatology, 7(6), 541-551.
23. Duan, Y., Ma, Z., & Yang, Q (2017) Characteristics of consecutive dry days variations in China. Theoretical and Applied Climatology, 130(1-2), 701-709.
24. Gaetani, M., Baldi, M., Dalu, G. A., Maracchi, G., Lionello, P., & Trigo, R (2011) Jetstream and rainfall distribution in the Mediterranean region. Natural Hazards & Earth System Sciences, 11(9).
25. Golian, S., Mazdiyasni, O., &AghaKouchak, A (2015) Trends in meteorological and agricultural droughts in Iran. Theoretical and applied climatology, 119(3-4), 679-688.
26. Griffith, D. A (2003) Spatial autocorrelation and spatial filtering: gaining understanding through theory and scientific visualization. Springer Science & Business Media.
27. Hosseinzadeh, S (2004) Environmental crises in the metropolises of Iran. WIT Trans. Ecol. Environ. 72.
28. Hosseinzadeh Talaee, P., Tabari, H., & Sobhan Ardakani, S (2014) Hydrological drought in the west of Iran and possible association with large-scale atmospheric circulation patterns. Hydrological Processes, 28(3), 764-773.
29. IPCC (2007) Climate change: synthesis report of the fourth assessment report. IPCC, Geneva
30. Johnson, N. C (2013) How many ENSO flavors can we distinguish?. Journal of Climate, 26(13), 4816-4827.
31. Lana X, Martinez MD, Burgueno A, Serra C, Martin-Vide J, Gomez L (2008) Spatial and temporal patterns of dry spell lengths in the Iberian Peninsula for the second half of the twentieth century. TheorApplClimatol 91:99–116
32. Llano, M. P., &Penalba, O. C (2011) A climatic analysis of dry sequences in Argentina. International journal of climatology, 31(4), 504-513
33. Kalnay, E., Kanamitsu, M., Kistler, R., Collins, W., Deaven, D., Gandin, L., ... & Zhu, Y (1996) The NCEP/NCAR 40-year reanalysis project. Bulletin of the American meteorological Society, 77(3), 437-472.
34. Kutiel H (1985) The multimodality of the rainfall course in Israel as reflected by the distribution of dry spells. ArchMetGeophBioclSer B39: 15–27
35. Kutiel H, Maheras P (1992) Variations Interannuelles des s_equencess_echeset des situations synoptiquesenM_editerrann_ee. Publications de l'AIC 5: 15–27
36. Mariotti, A (2007) How ENSO impacts precipitation in southwest central Asia. Geophysical Research Letters, 34(16).
37. Martin-Vide J, Gomez L (1999) Regionalization of peninsular Spain based on the length of dry spells. Int J Climatol 19:537–555

38. McCabe, G. J., Legates, D. R., &Lins, H. F (2010) Variability and trends in dry day frequency and dry event length in the southwestern United States. Journal of Geophysical Research: Atmospheres, 115(D7).
39. Min, S. K., Zhang, X., Zwiers, F. W., & Hegerl, G. C (2011) Human contribution to more-intense precipitation extremes. Nature, 470(7334), 378-381.
40. Mohammadrezaei, M., Soltani, S., & Modarres, R (2020) Evaluating the effect of ocean-atmospheric indices on drought in Iran. Theoretical and Applied Climatology, 140(1), 219-230.
41. Modarres, R (2006) Regional precipitation climates of Iran. J. Hydrol. (N. Z.) 13–27.
42. Modarres, R., &Sarhadi, A (2009) Rainfall trends analysis of Iran in the last half of the twentieth century. Journal of Geophysical Research: Atmospheres, 114(D3).
43. Moran, P. A (1950) Notes on continuous stochastic phenomena. Biometrika, 37(1/2), 17-23.
44. Najafi, M. R., &Moazami, S (2016) Trends in total precipitation and magnitude–frequency of extreme precipitation in Iran, 1969–2009. International Journal of Climatology, 36(4), 1863-1872.
45. Nasri, M., &Modarres, R (2009) Dry spell trend analysis of Isfahan Province, Iran. International Journal of Climatology: A Journal of the Royal Meteorological Society, 29(10), 1430-1438.
46. Nazaripour, H., &Daneshvar, M. M (2014) Spatial contribution of one-day precipitations variability to rainy days and rainfall amounts in Iran. International Journal of Environmental Science and Technology, 11(6), 1751-1758.
47. Nazemosadat, M. J., &Cordery, I (2000,a) On the relationships between ENSO and autumn rainfall in Iran. International Journal of Climatology: A Journal of the Royal Meteorological Society, 20(1), 47-61.
48. Nazemosadat, M. J., &Cordery, I (2000,b) The impact of ENSO on winter rainfall in Iran. Hydro 2000: Interactive Hydrology; Proceedings, 538.
49. Newman, M., Compo, G. P., & Alexander, M. A (2003) ENSO-forced variability of the Pacific decadal oscillation. Journal of Climate, 16(23), 3853-3857.
50. Oikonomou, C., Flocas, H. A., Hatzaki, M., Nisantzi, A., &Asimakopoulos, D. N (2010) Relationship of extreme dry spells in Eastern Mediterranean with large-scale circulation. Theoretical and applied climatology, 100(1-2), 137-151.
51. Raymond, F., Ullmann, A., Camberlin, P., Oueslati, B., & Drobinski, P (2018) Atmospheric conditions and weather regimes associated with extreme winter dry spells over the Mediterranean basin. Climate Dynamics, 50(11-12), 4437-4453.
52. Raziei, T., Mofidi, A., Santos, J. A., &Bordi, I (2012) Spatial patterns and regimes of daily precipitation in Iran in relation to large-scale atmospheric circulation. International Journal of Climatology, 32(8), 1226-1237.
53. Raziei, T., Daryabari, J., Bordi, I., & Pereira, L. S (2014) Spatial patterns and temporal trends of precipitation in Iran. Theoretical and applied climatology, 115(3-4), 531-540.
54. Schmidli, J., & Frei, C (2005) Trends of heavy precipitation and wet and dry spells in Switzerland during the 20th century. International Journal of Climatology: A Journal of the Royal Meteorological Society, 25(6), 753-771.
55. Sang, Y. W., Yik, D. J., Chang, N. K., & Yunus, F (2015) Analysis on the Long Term Trends of Consecutive Dry and Wet Days and Extreme Rainfall Amounts in Malaysia. Malaysian Meteorological Department.
56. Seleshi, Y., &Camberlin, P (2006) Recent changes in dry spell and extreme rainfall events in Ethiopia. Theoretical and Applied Climatology, 83(1-4), 181-191
57. Serra C, Burgueno A, Martinez MD, Lana X (2006) Trends in dry spells across Catalonia (NE Spain) during the second half of the20th century. TheorApplClimatol 85:165–183
58. Sezen, C., &Partal, T (2019) The impacts of Arctic oscillation and the North Sea Caspian pattern on the temperature and precipitation regime in Turkey. Meteorology and Atmospheric Physics, 131(6), 1677-1696.
59. Shenbrot, G.I., Krasnov, B.R., Rogovin, K.A (1999) Deserts of the world. In: Spatial Ecology of Desert Rodent Communities. Springer, pp. 5–24.
60. Singh, N., &Ranade, A (2010) The wet and dry spells across India during 1951–2007. Journal of Hydrometeorology, 11(1), 26-45
61. Sivakumar MVK (1992) Empirical analysis of dry spells for agricultural applications in west Africa. J Clim 5:532–539
62. Soulard, N., Lin, H., & Yu, B (2019) The changing relationship between ENSO and its extratropical response patterns. Scientific reports, 9(1), 1-10.

63. Some'e, B. S., Ezani, A., &Tabari, H (2012) Spatiotemporal trends and change point of precipitation in Iran. Atmospheric research, 113, 1-12.
64. Suppiah, R., & Hennessy, K. J (1998) Trends in total rainfall, heavy rain events and number of dry days in Australia, 1910–1990. International Journal of Climatology: A Journal of the Royal Meteorological Society, 18(10), 1141-1164.
65. Tabari, H., &Talaee, P. H (2011) Temporal variability of precipitation over Iran: 1966–2005. Journal of Hydrology, 396(3-4), 313-320
66. Unal, Y. S., Deniz, A., Toros, H., &Incecik, S (2012) Temporal and spatial patterns of precipitation variability for annual, wet, and dry seasons in Turkey. International Journal of Climatology, 32(3), 392-405.
67. Wang, H., Chen, Y., Pan, Y., & Li, W (2015) Spatial and temporal variability of drought in the arid region of China and its relationships to teleconnection indices. Journal of hydrology, 523, 283-296.
68. Wiedermann, M., Siegmund, J. F., Donges, J. F., & Donner, R. V (2021) Differential imprints of distinct ENSO flavors in global patterns of very low and high seasonal precipitation. Frontiers in Climate 3:618548.
69. Zhang, X., Zwiers, F. W., Hegerl, G. C., Lambert, F. H., Gillett, N. P., Solomon, S., ... &Nozawa, T (2007) Detection of human influence on twentieth-century precipitation trends. *Nature*, *448*(7152), 461-465.

Figures

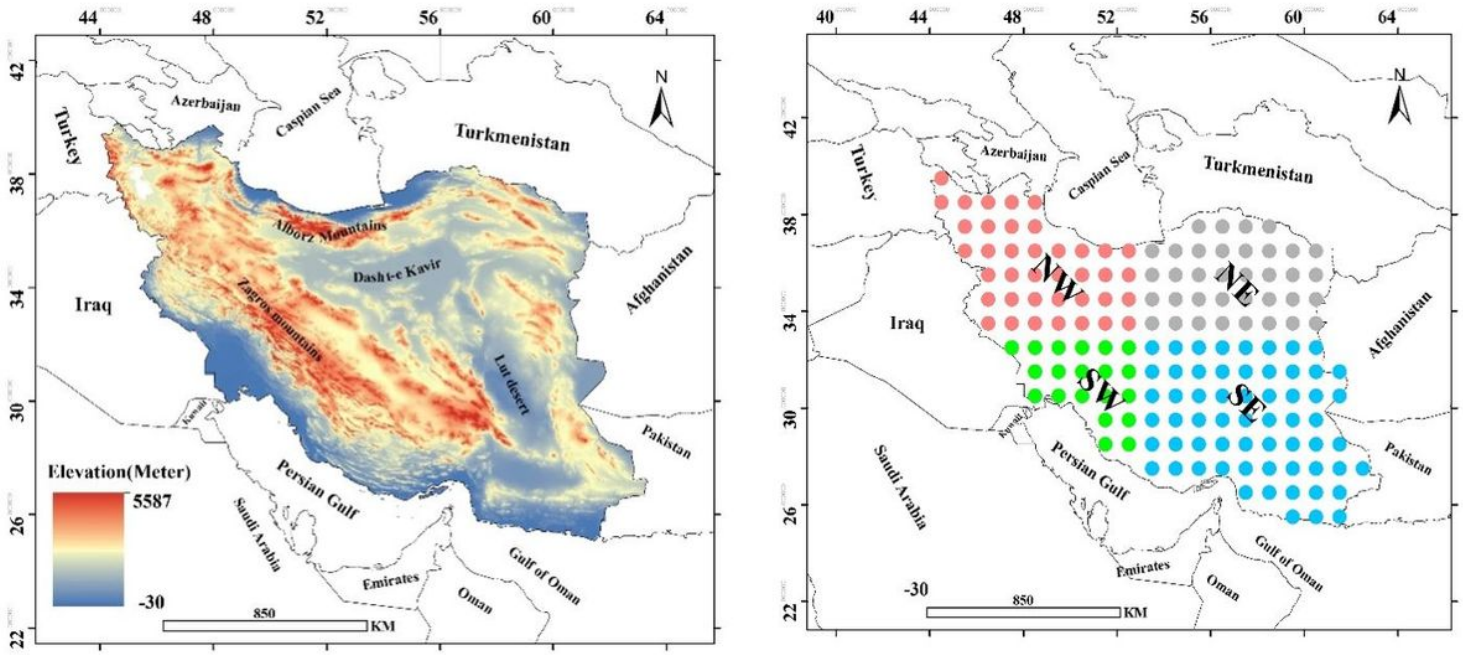

Figure 1

The geographical location of the study area. Topographic conditions (left panel) and classification of 1° latitude × 1° longitude points into different geographical areas (right panel). Note: The designations employed and the presentation of the material on this map do not imply the expression of any opinion whatsoever on the part of Research Square concerning the legal status of any country, territory, city or area or of its authorities, or concerning the delimitation of its frontiers or boundaries. This map has been provided by the authors.

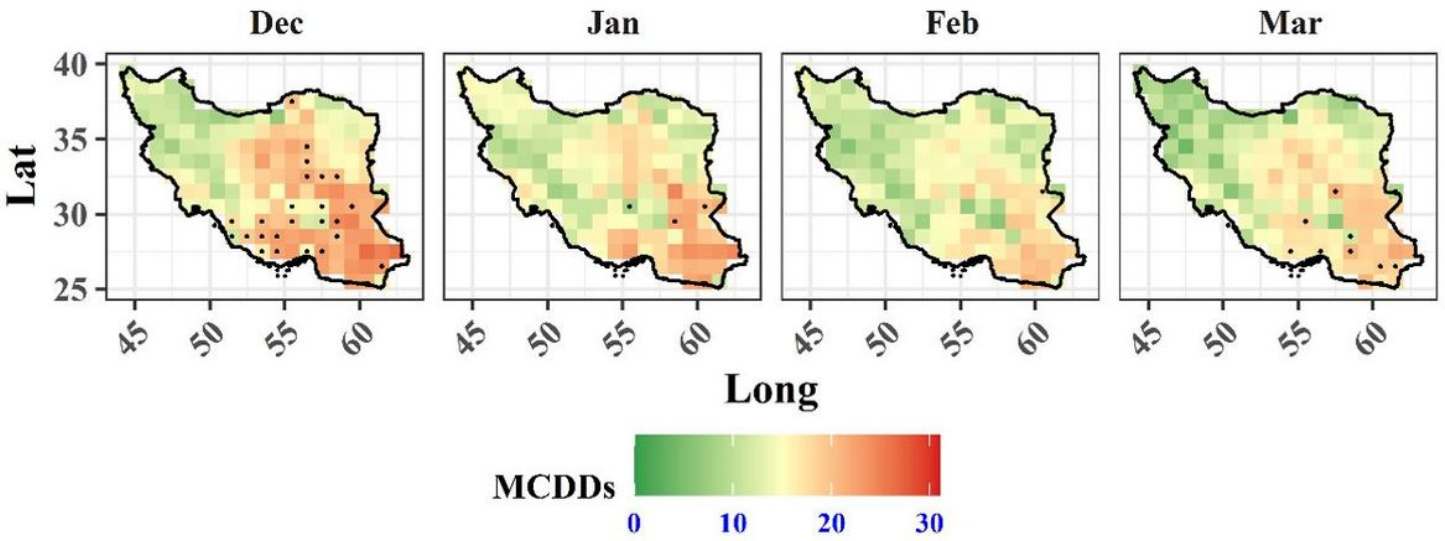

Figure 2

Spatial distribution of monthly average length of MCDDs during 1998-2019 over Iran (the marked grid points show points with relatively high standard deviation (above 8.) Note: The designations employed and the presentation of the material on this map do not imply the expression of any opinion whatsoever on the part of Research Square concerning the legal status of any country, territory, city or area or of its authorities, or concerning the delimitation of its frontiers or boundaries. This map has been provided by the authors.

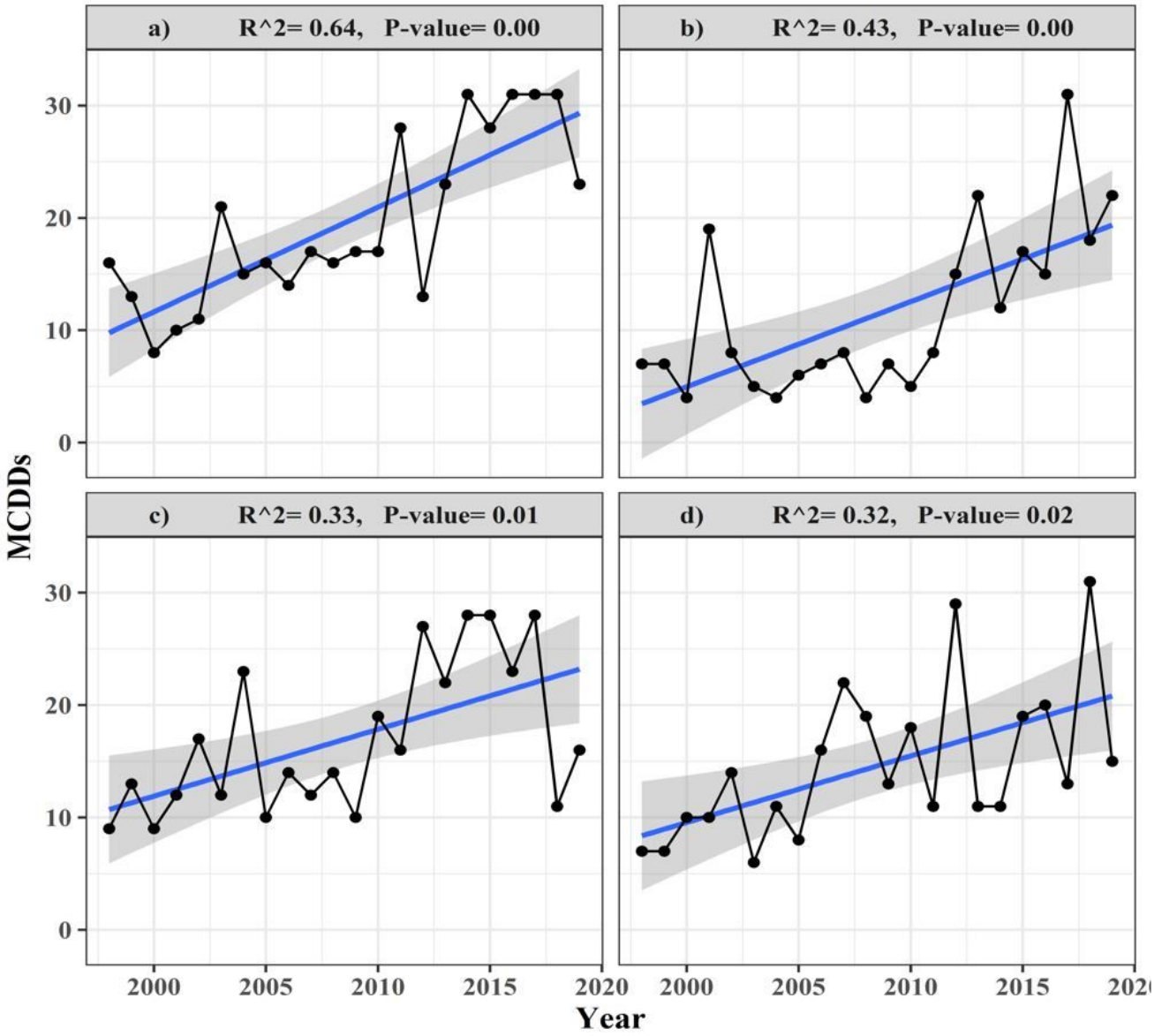

Figure 3

MCDDs trends for the gridpoints with the maximum coefficients of determination. a) At latitude 32.5° and longitude 54.5 °. b) At latitude 28.5° and longitude 51.5°. c) At latitude 34.5° and longitude 54.5. d) At latitude 33.5° and longitude 51.5 °. Note: The designations employed and the presentation of the material on this map do not imply the expression of any opinion whatsoever on the part of Research Square concerning the legal status of any country, territory, city or area or of its authorities, or concerning the delimitation of its frontiers or boundaries. This map has been provided by the authors.

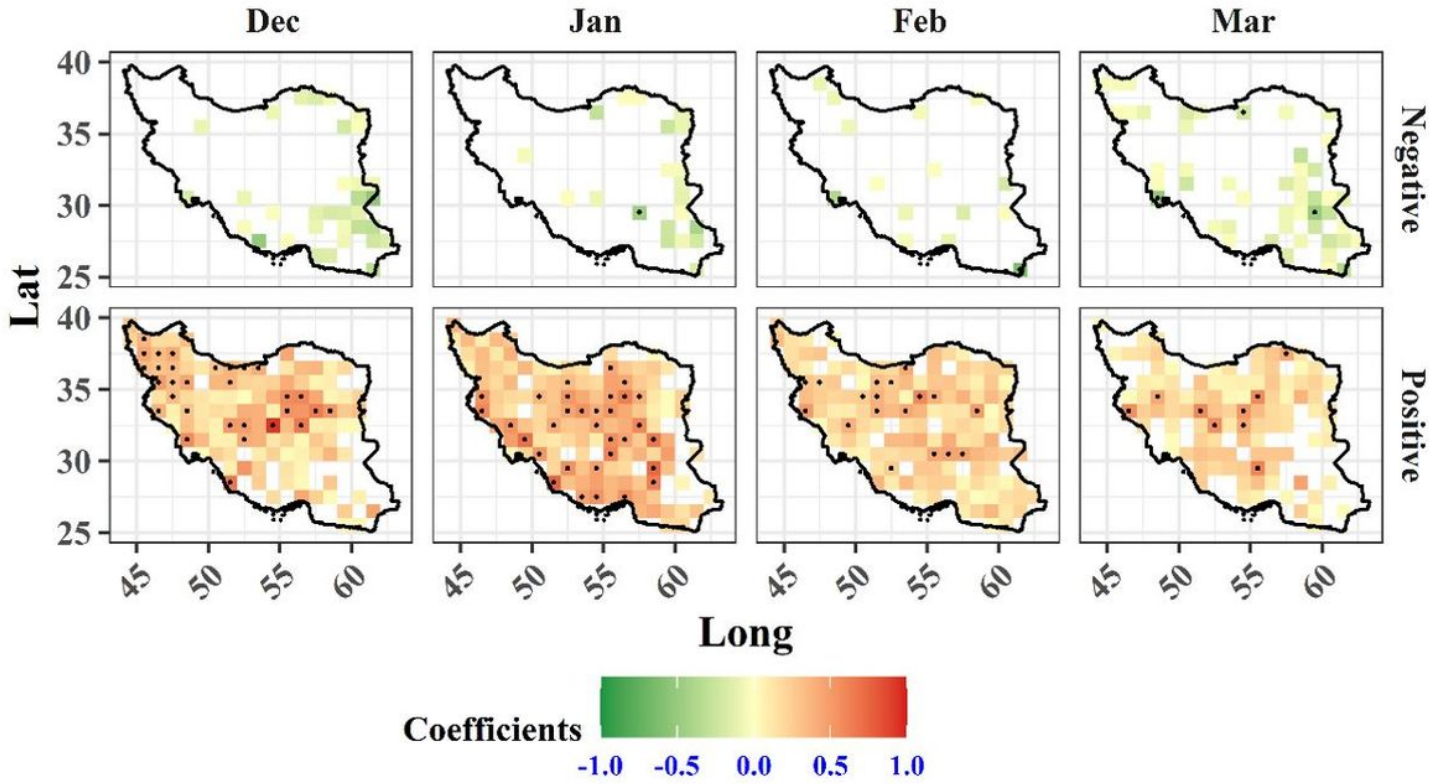

Figure 4

Spatial distribution of monthly negative (top row) and positive (bottom row) MCDDs linear trend during 1998-2019 over Iran (the marked grid points show a statistically significant coefficient for $p < 0.05$). Note: The designations employed and the presentation of the material on this map do not imply the expression of any opinion whatsoever on the part of Research Square concerning the legal status of any country, territory, city or area or of its authorities, or concerning the delimitation of its frontiers or boundaries. This map has been provided by the authors.

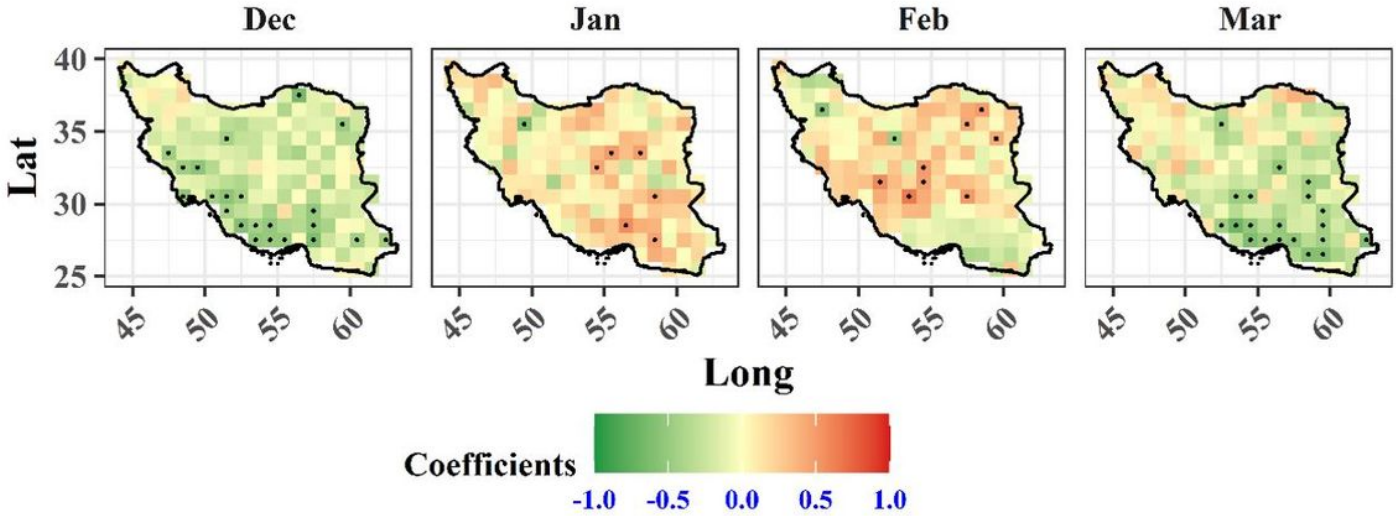

Figure 5

The correlation coefficients between MCDDs values and ENSO separately for December to March (The marked grid points show a statistically significant coefficient for $p < 0.05$). Note: The designations employed and the presentation of the material on this map do not imply the expression of any opinion whatsoever on the part of Research Square concerning the legal status of any country, territory, city or area or of its authorities, or concerning the delimitation of its frontiers or boundaries. This map has been provided by the authors.

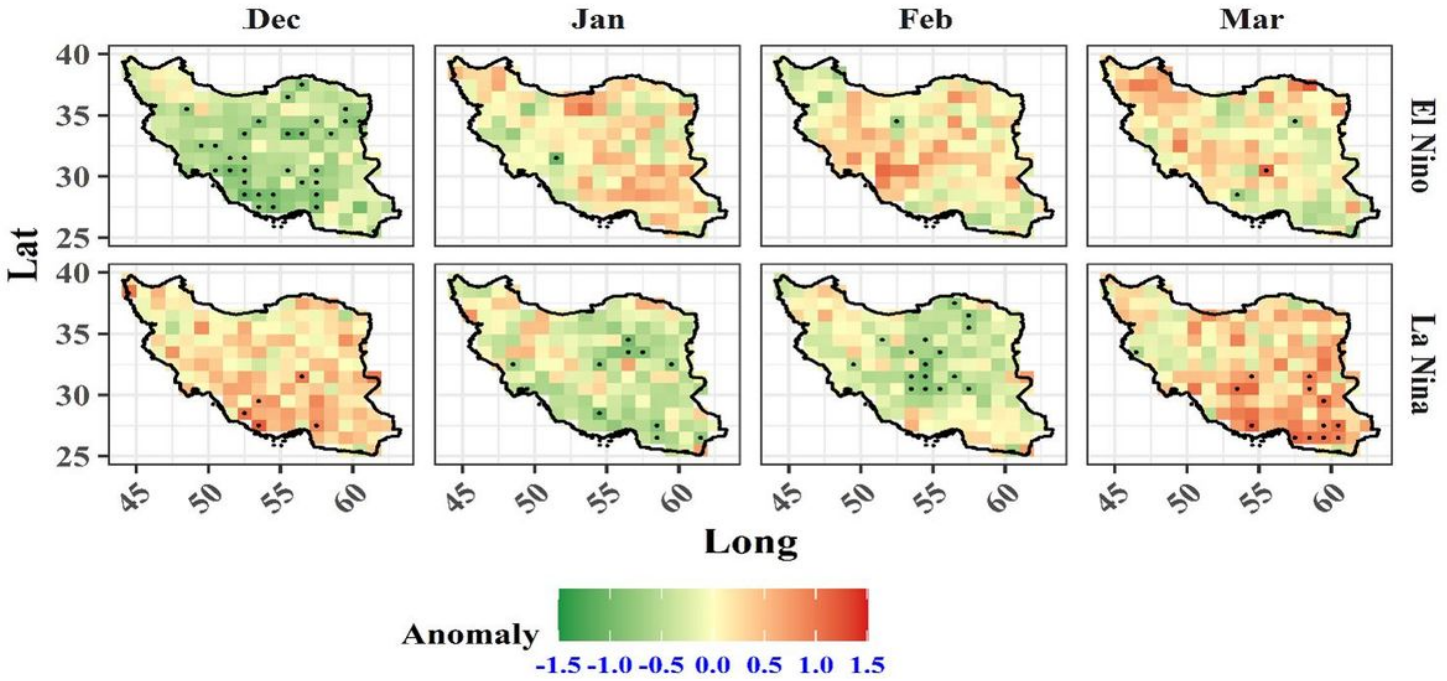

Figure 6

Comparison of MCDDs anomalies in five years of positive and five years of negative phases of the ENSO index. Top row El Niño , bottom row La Niña. Marked grid points show statistically significant differencs for $p < 0.05$ based on t-test when comparing El Niño (La Niña) with all years. Note: The designations employed and the presentation of the material on this map do not imply the expression of any opinion whatsoever on the part of Research Square concerning the legal status of any country, territory, city or area or of its authorities, or concerning the delimitation of its frontiers or boundaries. This map has been provided by the authors.

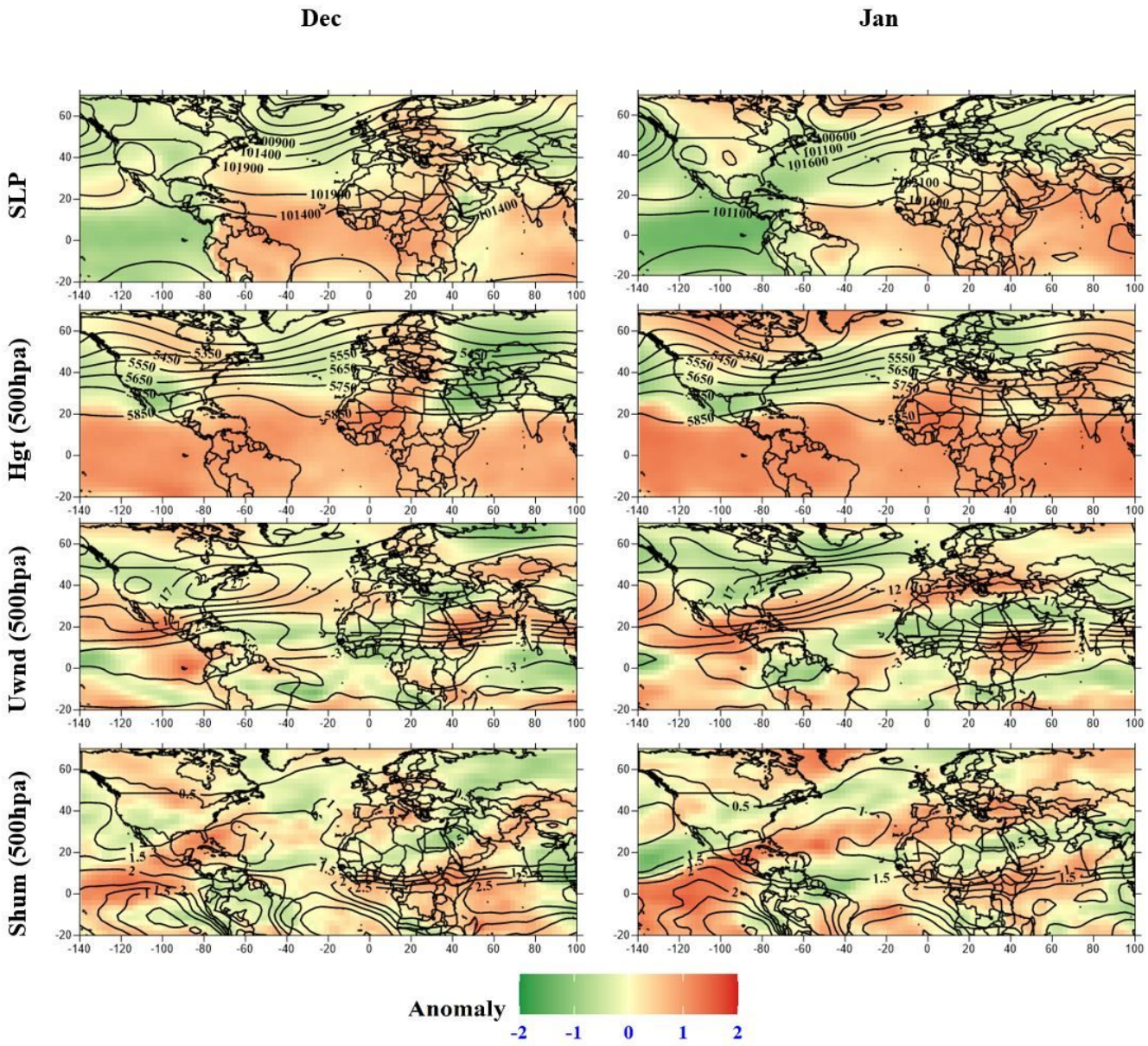

Figure 7

Comparison of anomaly values of large-scale atmospheric variables in El Niño phases between December (left panel) and January (right panel). Note: The designations employed and the presentation of the material on this map do not imply the expression of any opinion whatsoever on the part of Research Square concerning the legal status of any country, territory, city or area or of its authorities, or concerning the delimitation of its frontiers or boundaries. This map has been provided by the authors.

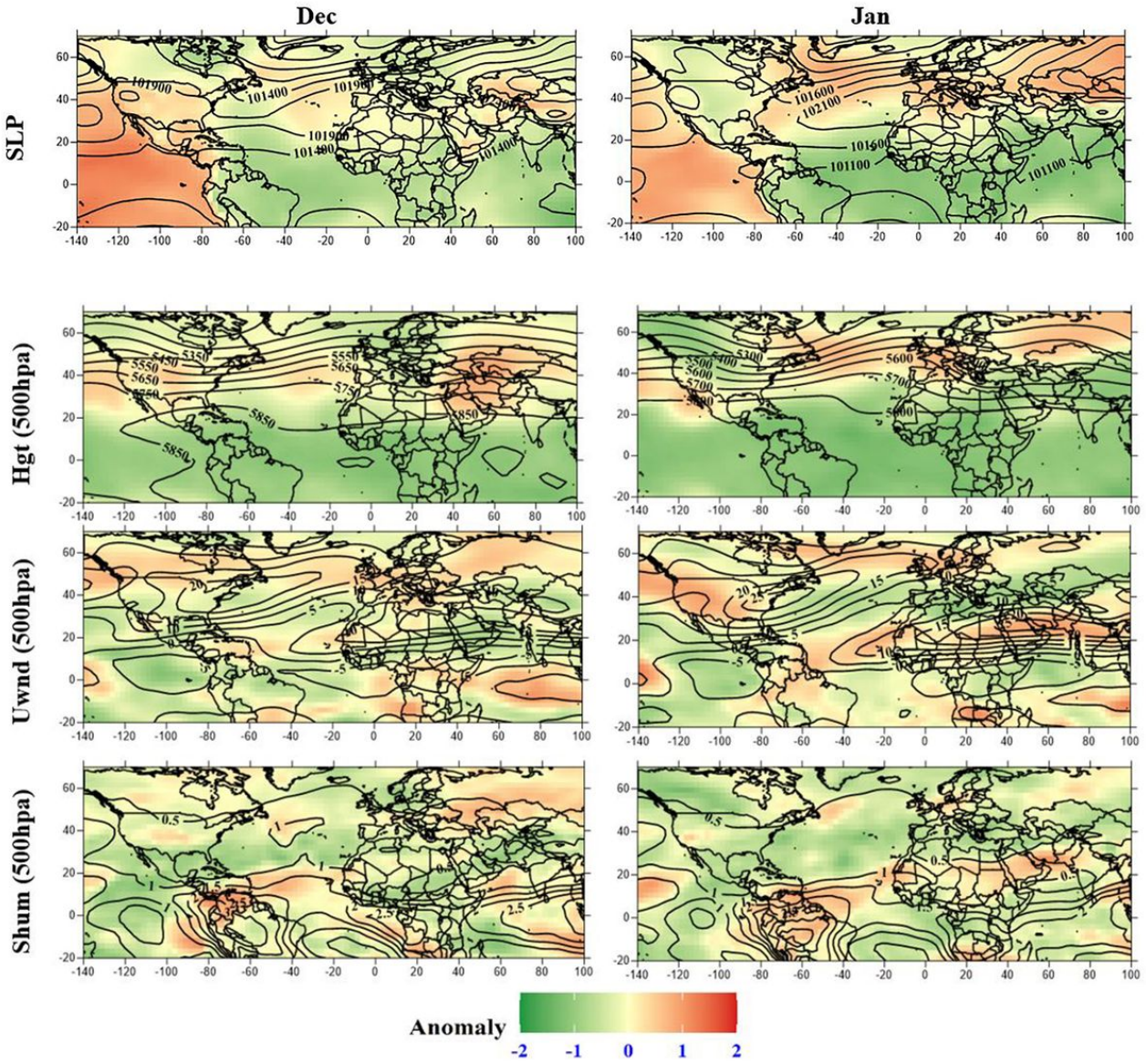

Figure 8

Comparison of anomaly values (color shading) of large-scale atmospheric variables in LaNiña phases between December (left panel) and January (right panel).

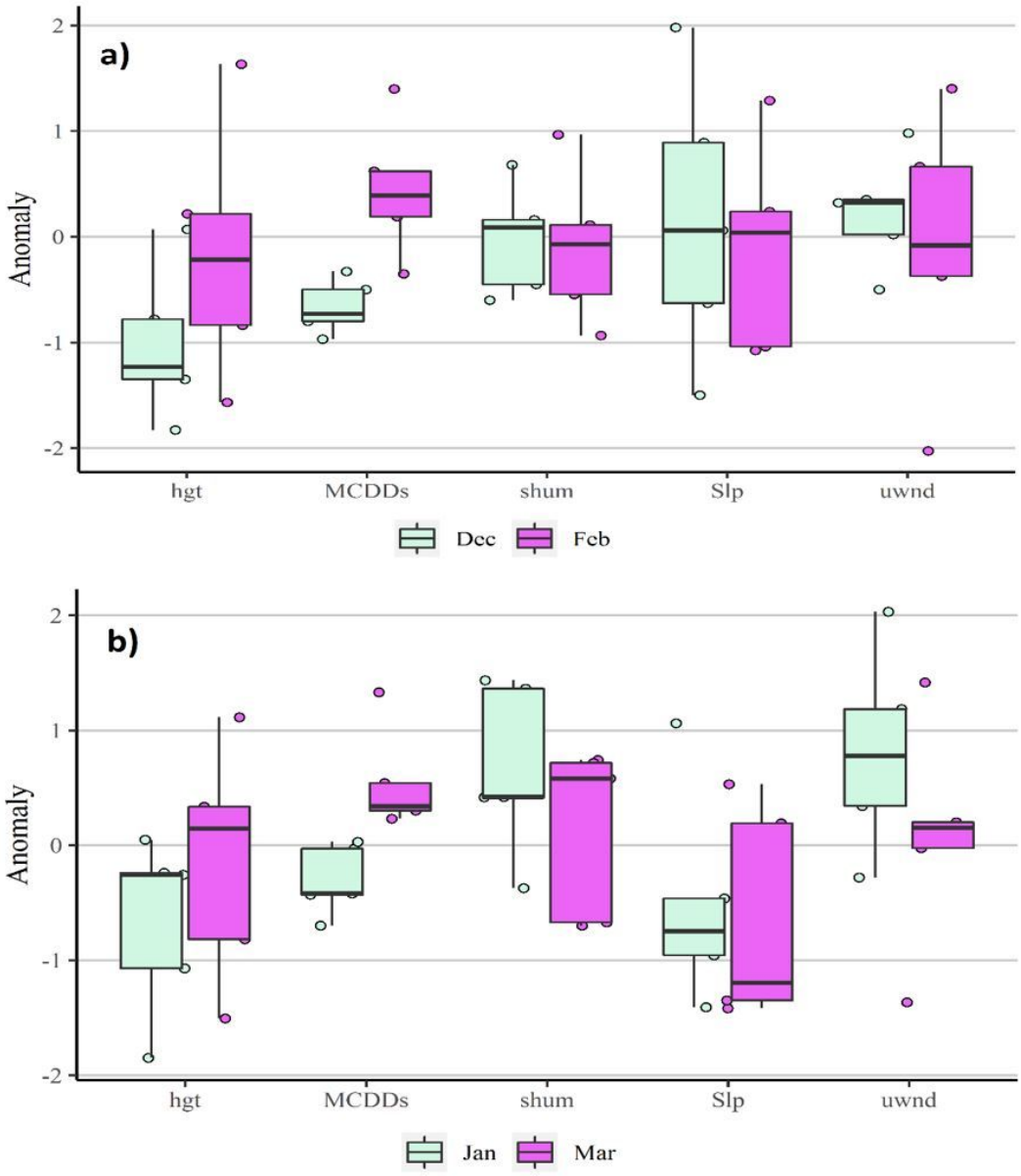

Figure 9

Boxplots of MCDDs and atmospheric variables anomalies during the La Niña and El Niño years a) in December during El Niño years at southwest (green color boxes) and in February during El Niño years at southwest (violet color boxes). b) in January during La Niña years at southeast (green color boxes) and in March during La Niña years at southeast (violet color boxes). Dots represent the 5 strongest El Niño and La Niña years (see Table 1). Note: The designations employed and the presentation of the material on this map do not imply the expression of any opinion whatsoever on the part of Research Square concerning the legal status of any country, territory, city or area or of its authorities, or concerning the delimitation of its frontiers or boundaries. This map has been provided by the authors.

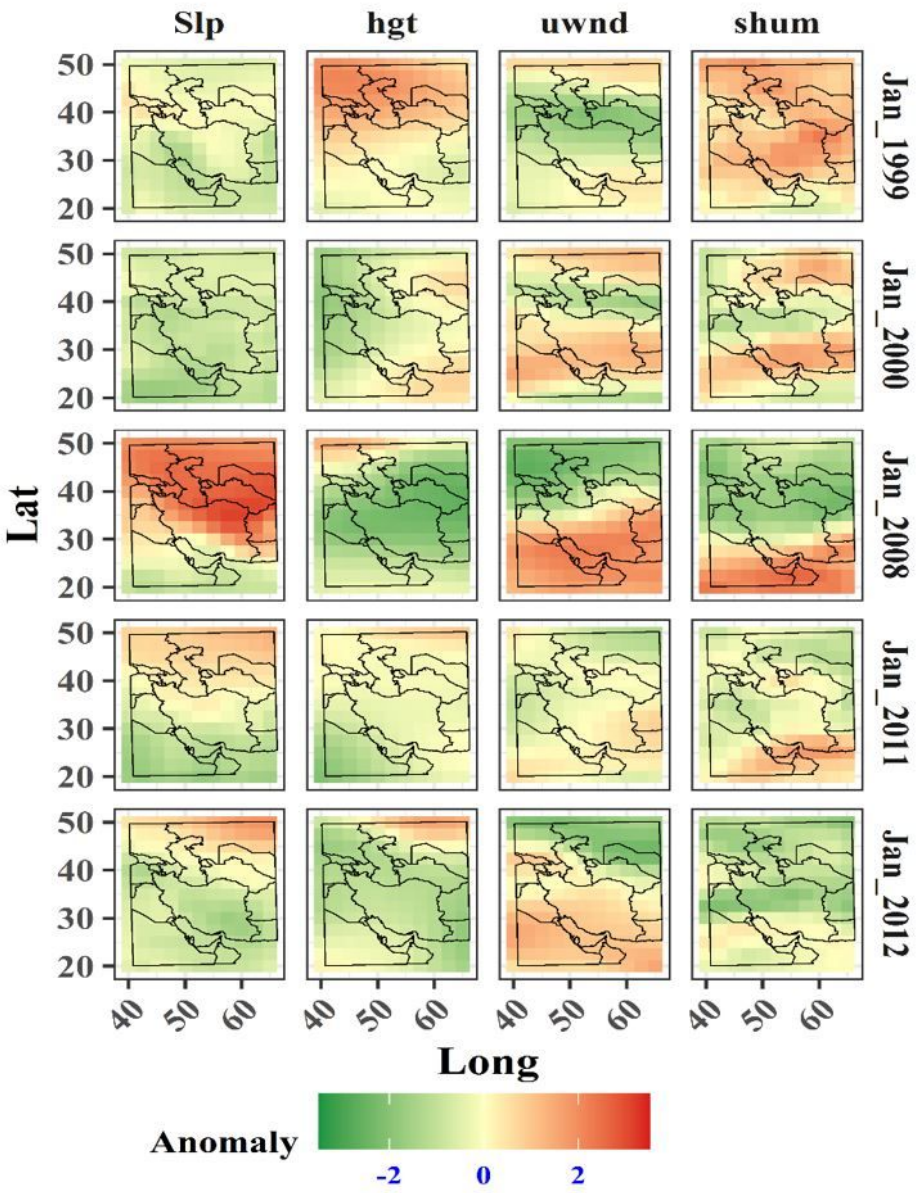

Figure 10

The anomalous values of atmospheric variables during January in each of the La Niña years separately. Note: The designations employed and the presentation of the material on this map do not imply the expression of any opinion whatsoever on the part of Research Square concerning the legal status of any country, territory, city or area or of its authorities, or concerning the delimitation of its frontiers or boundaries. This map has been provided by the authors.

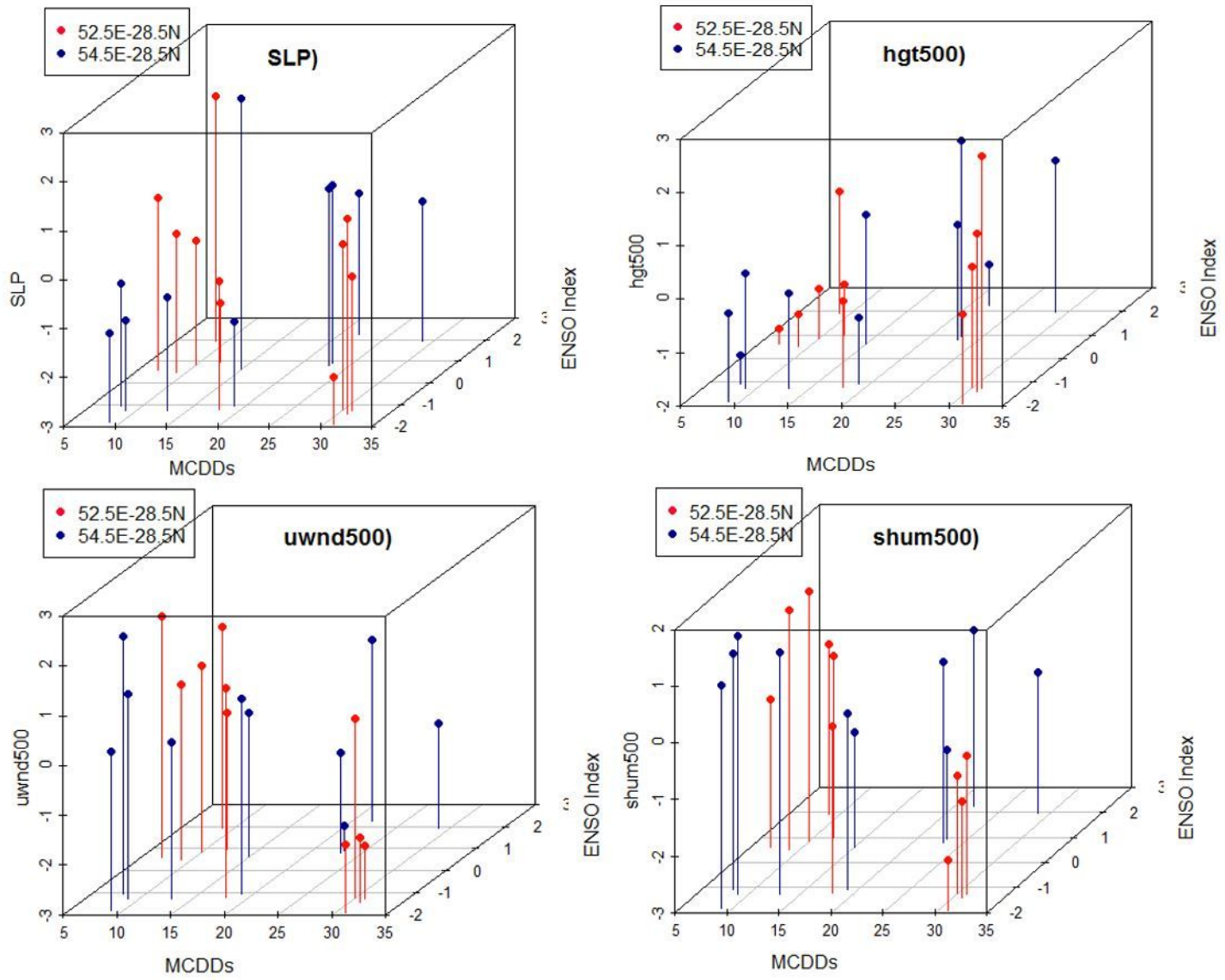

Figure 11

Three-dimensional scatter plots of ENSO, MCDDs, and atmospheric variables in the two points in January (54.5E_28.5N, blue colour) and December (52.5E_28.5N, red colour) in El Niño and La Niña phases.

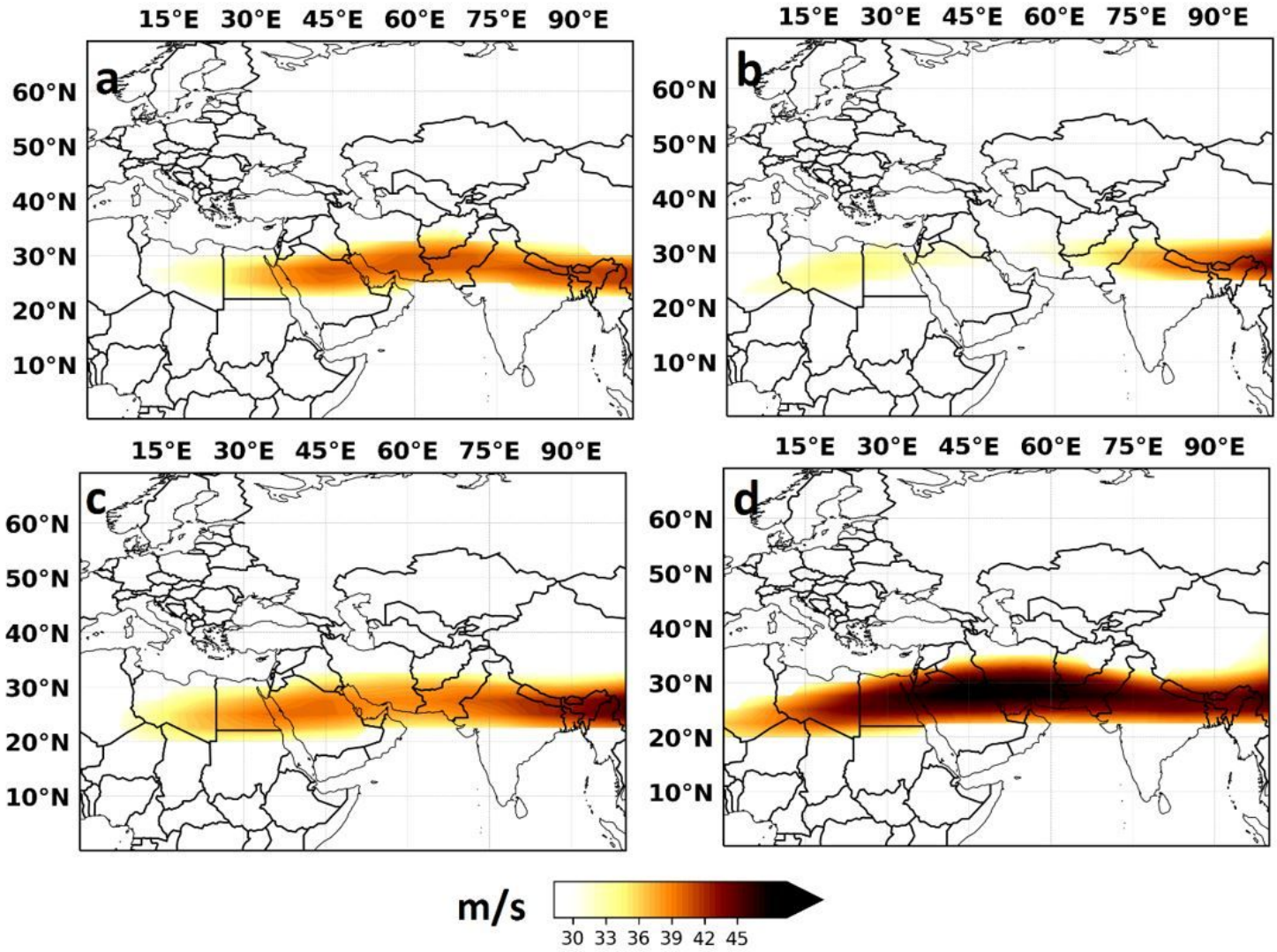

Figure 12

Comparison of jetstream patterns at 300-hPa in the El Niño and La Niña years. a) December - El Niño years. b) December – La Niña years. c) January - El Niño years. d) January – La Niña years. Note: The designations employed and the presentation of the material on this map do not imply the expression of any opinion whatsoever on the part of Research Square concerning the legal status of any country, territory, city or area or of its authorities, or concerning the delimitation of its frontiers or boundaries. This map has been provided by the authors.